BBA - Biomembranes xxx (xxxx) xxx–xxx

Contents lists available at ScienceDirect

BBA - Biomembranes

journal homepage: www.elsevier.com/locate/bbamem

Luminescence resonance energy transfer spectroscopy of ATP-binding cassette proteins☆

Maria E. Zoghbi[a], Guillermo A. Altenberg[b,*]

[a] School of Natural Sciences, University of California, Merced, 4225 N. Hospital Road, Atwater, CA, USA
[b] Department of Cell Physiology and Molecular Biophysics, and Center for Membrane Protein Research, Texas Tech University Health Sciences Center, Lubbock, TX 79423-6551, USA

ARTICLE INFO

Keywords:
P-glycoprotein
MsbA
LRET
FRET
Fluorescence
NBD

ABSTRACT

The ATP-binding cassette (ABC) superfamily includes regulatory and transport proteins. Most human ABC exporters pump substrates out of cells using energy from ATP hydrolysis. Although major advances have been made toward understanding the molecular mechanism of ABC exporters, there are still many issues unresolved. During the last few years, luminescence resonance energy transfer has been used to detect conformational changes in real time, with atomic resolution, in isolated ABC nucleotide binding domains (NBDs) and full-length ABC exporters. NBDs are particularly interesting because they provide the power stroke for substrate transport. Luminescence resonance energy transfer (LRET) is a spectroscopic technique that can provide dynamic information with atomic-resolution of protein conformational changes under physiological conditions. Using LRET, it has been shown that NBD dimerization, a critical step in ABC proteins catalytic cycle, requires binding of ATP to two nucleotide binding sites. However, hydrolysis at just one of the sites can drive dissociation of the NBD dimer. It was also found that the NBDs of the bacterial ABC exporter MsbA reconstituted in a lipid bilayer membrane and studied at 37 °C never separate as much as suggested by crystal structures. This observation stresses the importance of performing structural/functional studies of ABC exporters under physiologic conditions. This article is part of a Special Issue entitled: Beyond the Structure-Function Horizon of Membrane Proteins edited by Ute Hellmich, Rupak Doshi and Benjamin McIlwain.

1. Introduction

Membrane proteins (MPs) constitute between 20 and 30% of the sequenced genomes, and are the targets of > 50% of pharmacological agents in the market [1]. Alterations in MP function of genetic and acquired origin are at the core of disorders of medical importance such as cystic fibrosis, cerebrovascular accidents, deafness, cardiac infarcts, and neurodegenerative diseases, among many. Since MPs mediate fundamental life processes, they are of broad interest to the basic sciences as well as to the fields of biotechnology and medicine. Despite the relevance of MP, understanding their structure and function has been limited by the experimental difficulties associated with the heterogeneous lipid/water environment where these proteins reside. Therefore, it is of great interest to develop experimental approaches that can allow us to study MP in their natural environment.

Most high-resolution structures of MPs have been obtained by X-ray crystallography and to a much lesser extent by NMR spectroscopy. Cryo-electron microscopy/single-particle analysis has emerged as a powerful methodology that has produced a number of recent structures; it is expected that it will soon rival or surpass X-ray crystallography as a source of membrane protein structures, including structures in MPs in the membrane. In some cases, it is possible to obtain high-resolution structures of proteins "locked" in different conformations directly or by a hybrid approach combining a structure in a particular conformation with experimental data and computational modeling. Examples are the uses of electron paramagnetic resonance spectroscopy to obtain data of proteins locked in different conformations using site-directed spin labeling in combination with either continuous wave-electron paramagnetic resonance spectroscopy (side chain environment and dynamics) or double electron-electron resonance (DEER) spectroscopy (spin label-spin label distances). High-resolution structures and information on proteins locked in specific states are essential to understand how proteins work because they provide a detailed picture of the proteins "frozen" in a particular conformation. However, proteins are highly flexible molecules that sample an ensemble of conformations around the average structure because of thermal motion. They also

☆ This article is part of a Special Issue entitled: Beyond the Structure-Function Horizon of Membrane Proteins edited by Ute Hellmich, Rupak Doshi and Benjamin McIlwain.

* Corresponding author.
E-mail address: g.altenberg@ttuhsc.edu (G.A. Altenberg).

http://dx.doi.org/10.1016/j.bbamem.2017.08.005
Received 2 June 2017; Received in revised form 31 July 2017; Accepted 1 August 2017

experience slow molecular motions in the microsecond to second timescale. These are low probability events that lead to higher energy states on an energy landscape, which are directly linked to protein function. It follows that understanding the mechanisms of proteins at the atomic/molecular level requires a description of the conformational states and the kinetics of the essential transitions between those states. This cannot be achieved only with high-resolution structures of defined states, but requires protein dynamics studies that add a time dimension to the high-resolution structural snapshots.

Optical spectroscopic techniques such as Förster (or fluorescence) resonance energy transfer (FRET) and luminescence resonance energy transfer (LRET) are ideal to follow conformational changes in real time under physiological conditions. They can provide information at the population (*e.g.*, FRET, LRET, Trp fluorescence spectroscopy) and single-molecule levels (*e.g.*, single-molecule FRET). FRET and LRET have atomic-resolution and high sensitivity, and can provide dynamic information on the most relevant conformational changes of membrane proteins that are associated with function. FRET has been a methodology of choice for dynamics studies in the ns to s time range. However, light scattering by detergent micelles and liposomes complicates FRET quantitation in membrane-protein studies. Light-scattering problems are minimized when LRET is used instead of FRET to follow membrane-protein domain motions, although these motions have to be generally slower than 200 μs.

In this review, we discuss our recent findings using luminescence spectroscopy to study ATP-binding cassette (ABC) transporters. We present examples of the use of Trp spectroscopy and LRET to study ABC proteins under steady-state conditions and during transitions between defined states. We frequently refer to publications that deal with specific issues, where more extensive references and original publications are included.

2. Membrane-protein platforms

2.1. Traditional membrane-protein platforms

Purification and reconstitution are critical to study the structure and function of MPs under well-controlled experimental conditions. However, whereas working with purified proteins is essential for most detailed structural studies of MPs, functional, and also structural studies of MPs have been successfully performed with proteins in membrane vesicles. One clear advantage of this type of studies is that the MPs are studied in their native membrane environment. As an example, an approach for transport studies of ABC exporters is the use of inside-out membrane vesicles with measurements of ATP-dependent substrate uptake upon addition the nucleotide to the bath [2]. For the work with purified MPs, an essential step is the extraction of the proteins from cell membranes with amphiphiles. Solubilization of membranes with detergents is the most frequent approach because of the availability of a broad range of detergents with different properties and the simplicity of the process. However, detergent micelles have very different physicochemical properties than lipid bilayers, which contribute to the reduced stability of detergent-solubilized MPs. Lipids have a major contribution to the curvature, lateral pressure profile, thickness, and other bulk physicochemical properties of biomembranes [3–6]. While these properties are generally preserved in artificial lipid bilayers, they are largely absent in detergent, detergent-mimicking alternatives such as peptide surfactants, amphipols, and facial amphiphiles [7–9]. Bicelles are discoidal structures formed by phospholipids and detergent, with a planar region that mimics a biomembrane [10]. Unfortunately, bicelles can only be formed with limited lipid compositions and knowledge of the properties of MPs in bicelles *vs*. MPs in lipid bilayer is very limited.

Reconstitution of detergent-solubilized MPs into lipid bilayers increases their stability, and unilamellar liposomes represent a well-established reconstitution configuration. The lipid bilayer of liposomes separates two compartments, making liposomes well suited for membrane transport studies. However, since the accessibility to the intraliposomal side is limited, the use of liposomes represents a complication for applications such as binding studies. In addition, the relatively large size of the liposomes complicates optical spectroscopy measurements due to light scattering. In recent years, nanodiscs (NDs) have been introduced as a new approach for the study of membrane proteins in a lipid bilayer. NDs are proteolipid or polymer-lipid nanostructures that display a great potential as platforms for the study of MPs [11–13].

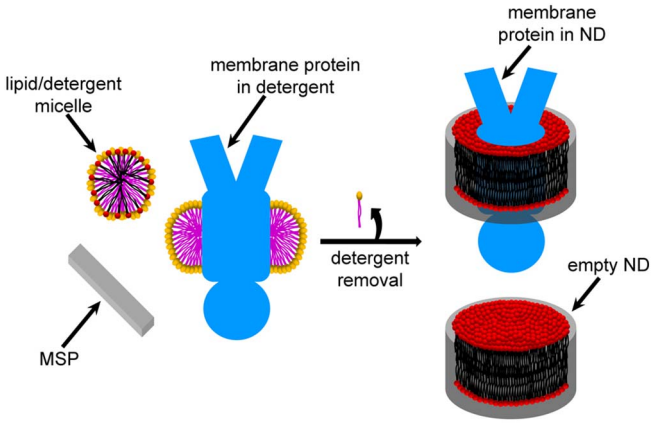

Fig. 1. Self-assembly of nanodiscs (NDs). Schematic representation of the formation of NDs upon detergent removal from a mixture containing membrane scaffold protein (MSP) and detergent-solubilized phospholipids and membrane proteins. Detergent molecules are represented as yellow ovals (hydrophilic heads) with magenta tails (hydrophobic moieties), and phospholipids as red circles (hydrophilic heads) and black tails (hydrophobic chains).

2.2. Nanodiscs

NDs consist of two molecules of a membrane scaffold protein (MSP) that encase a small patch of lipid bilayer (Fig. 1) [12,13]. Most MSPs are based on apolipoprotein A1, a major component of serum high-density lipoprotein complexes [13]. Changing the MSP length allows for control of the NDs size in the ~8–17 nm range [12–15], which can be useful to adapt diameter to the application. In the NDs, most hydrophobic residues of the MSPs interact with the hydrophobic moiety of the lipid bilayer, whereas the MSPs hydrophilic residues face the outside and help to maintain the solubility of the NDs in water-based solutions [12,13,16].

Upon detergent removal, NDs assemble spontaneously from mixtures containing MSP and detergent-solubilized lipids (Fig. 1) [13,14,17]. Possibilities to remove the detergent include dialysis, detergent-binding columns, and binding to detergent-absorbing beads such as Bio-Beads SM2 from Bio-Rad [12–14,18]. Varied MPs have been incorporated in NDs of varied lipid compositions [12–14,18]. The appropriate phospholipid:MSP molar ratio depends on the length of the MSP (ND diameter) and the absence or presence of MP. Incorrect ratios can lead to low reconstitution efficiency, MSP aggregation and/or formation of large proteolipid complexes [14,18].

Styrene-maleic acid (SMA)-lipid particles (SMALPs) or Lipodisqs are a relatively recent ND variation. SMALPs are polymer-encased NDs where amphipathic SMA copolymers replace the MSPs [19–21]. The interest in SMALPs is increasing for two main reasons. One is that SMA copolymers act as a membrane solubilisation agent, generating NDs directly from biological membranes [19–21], bypassing the use of detergent, which can be disruptive for many MPs, and the reconstitution step. The other reason is that SMALPs made from solubilisation of native membranes contain the original lipids, which may be an advantage to study MPs in a close to physiological environment [19–21]. Significant disadvantages are the poor control of SMALPs diameter and the

incompatibility of SMA with common buffer solutions (low pH, cationic solutes) [19,22,23]. The latter include coordination of the SMA carboxylates with the immobilized metals used to purify His-tagged MPs, and precipitation due to electrostatic interaction between the SMA carboxylates and divalent inorganic cations. Relevant to ABC proteins, their ATPase activity requires Mg^{2+}, precluding studies of functional ABC proteins reconstituted in SMALPs. Recent finding and future developments are likely to address the problems described and increase the use of SMALPs [24].

3. Lanthanide-based (or luminescence) resonance energy transfer (LRET)

3.1. Basic principles of LRET

FRET and LRET are two sensitive spectroscopic techniques based on energy transfer from a donor to an acceptor. Energy transfer between the donor and acceptor depends on the distance that separates these spectroscopic probes, making these techniques very useful for the study of conformational changes in proteins. FRET and LRET are particularly well suited for structural studies of biomolecules because efficient energy transfer occurs in a distance range compatible with the size of biological macromolecules and membrane thickness, and its extent can be predicted from the donor-acceptor distance and the properties of the donor and acceptor [25]. FRET occurs between a donor molecule in the excited state and an acceptor molecule in the ground state. Generally, the donor emits light at wavelengths that overlap with the acceptor absorption spectrum. However, energy transfer does not occur through photons emitted by the donor, but it is the result of long range dipole-dipole interactions between the donor and acceptor. This is important because photons can travel very long distances and absorption does not depend intrinsically on the distance, but on many factors that include concentration of the molecule that absorbs and pathlength. LRET is somewhat similar to the traditional FRET, but in LRET a luminescent lanthanide (generally Tb^{3+} or Eu^{3+}) chelate is used as donor [26]. Tb^{3+} and Eu^{3+} display long lifetime of their excited states because emission arises from a parity forbidden 4*f* to 4*f* electronic transition that also involves a high spin to high spin transition from an S = 2 state ($^5D_4$ for Tb^{3+} and $^5D_0$ for Eu^{3+}) to an S = 3 state (^7F_J, where J = 0–6) [26]. Because of the high spin nature of the transitions, emission of the luminescent lanthanides is not formally fluorescence (singlet-to-singlet transition) or phosphorescence (triplet-to-singlet transition) [25,26]. However, since emission arises primarily from electric dipole transitions [26], the electric field produced by Tb^{3+} or Eu^{3+} and by a FRET organic donor have the same dependence on distance (R), decreasing as a function of R^{-3} (for $R \ll \lambda$) resulting in the same dependence on distance (R^{-6}) for FRET and LRET.

LRET has a number of advantages over FRET for studies of MPs. These advantages are the result of two unique properties of the luminescent lanthanides, namely line spectra emission and long lifetime of the excited state. Different from the broad spectra of traditional fluorophores used in FRET, Tb^{3+} and Eu^{3+} chelates display atomic-like line spectra, with sharp peaks separated by dark regions (Fig. 2A). This permits isolation of the acceptor fluorophore emission without contamination from donor emission. Avoiding overlap between the broad excitation and emission spectra of the donor and acceptor in FRET is not possible. Also, lifetimes of the excited-state of traditional fluorophores are generally in the ns range (*e.g.*, ~3 ns for fluorescein), whereas those of Tb^{3+} and Eu^{3+} are 10^5 to 10^6 folds longer, in the ms range [25,26]. The long lifetime of the Tb^{3+} and Eu^{3+} excited states can be used to introduce a delay between a relatively short excitation pulse and the acquisition of the acceptor emission [26,27]. In this acquisition mode, the detector is off during the excitation pulse and is gated-on with a delay of tens to hundreds of μs from the excitation pulse (Fig. 2B). In practice, the LRET donor is excited with a relatively short pulse from a laser or a flash lamp, and the long-lifetime emission is recorded with a 20–200 μs delay after the excitation pulse. The LRET donor and the acceptor sensitized emission arising from LRET are recorded. The sensitized LRET emission is the long-lifetime emission from the LRET acceptor that can only originate from energy transfer from Tb^{3+} or Eu^{3+} chelates to traditional fluorophores [26]; for example, the intrinsic lifetime of fluorescein emission is ~3 ns, whereas the sensitized emission of a fluorescein acceptor has a ms lifetime because the fluorescein acceptor follows the long-lifetime emission from the LRET donors that participate in LRET. During the delay, before the detector is gated-on, light from processes with lifetimes in the ns range will decay to negligible values, resulting in a very low background. These processes include sample autofluorescence, emission due to direct excitation of the acceptor, and scattering of the excitation pulse [26]. Light scattering is a major problem in spectroscopic research of MPs in liposomes, detergent micelles, and NDs. Another advantage of LRET is that the emission from the donor and acceptor is unpolarized [26,28]. This reduces problems due to orientation factors, which introduce uncertainties in FRET-based calculations (see Section 3.3). Also different from FRET, donor-acceptor distances calculated from sensitized emission lifetimes are independent of the labeling stoichiometry [26,29]. When using chemical labeling probes in LRET, the signals from donors and acceptors that are unpaired and do not participate in energy transfer have to be subtracted. In contrast, since in LRET the sensitized emission originates exclusively from energy transfer, it is not necessary to subtract emission from donors and acceptors that do not participate in energy transfer. The increase in LRET donor-acceptor pairs will improve sensitivity, but will not have effect on LRET calculations.

3.2. Lanthanide probes

Luminescent Tb^{3+} or Eu^{3+} chelate complexes are used as donors in LRET. They have ms lifetimes and high quantum yields, and produce unpolarized sharp atomic-like line emission spectra with a broad visible emission range that extends from ~490 to 700 nm [26]. To assess conformational changes in proteins using LRET, efficient excitation of the donor and control of the position of the Tb^{3+} or Eu^{3+} chelates in the protein are essential. Because of their low absorption coefficients (< 1000 folds of organic fluorophores), the luminescent lanthanides are rarely excited directly, but their excitation is mediated by a nearby antenna of high absorption coefficient. Lanthanide excitation in the chelate is accomplished in a two-step process where the excitation light is first absorbed by the antenna (step 1 in Fig. 2C and D), which in turn transfers energy to the lanthanide with high efficiency (step 2 in Fig. 2C and D). The emission quantum yield for Tb^{3+} and Eu^{3+} in the chelates used for LRET is quite high, which is important because of the dependence of energy transfer efficiency on the donor quantum yield [26,30]. Lanthanide complexes include those where the chelator and antenna are distinct components, and those where the chelate backbone coordinates the lanthanide and serves as antenna. The first group includes the lanthanide chelate DTPA-cs124-EMCH that we have used (Fig. 2C) [30]. The second group includes organic compounds such as pyridine derivatives and the genetically-encoded lanthanide binding tags (Fig. 2D) [26,31–34].

In addition to an efficient excitation, an accurate positioning of the luminescent lanthanide chelates is required. The most common approach is the use recombinant proteins with Cys residues that can be selectively labeled by standard thiol chemistry, generally using maleimides or methanethiosulfonates. Although not always necessary, all native Cys can be replaced to generate a functional Cys-less protein that can then be used as framework to introduce Cys in the places desired for the location of the LRET probes. The time invested to reach this point varies from protein to protein and it is difficult to predict. In our experience, it was relatively simple to do it for the ABC bacterial exporter MsbA because substitution of all native Cys residues with Ala and/or Ser yielded a fully-functional protein [35]. In contrast, to develop a fully-functional Cys-less P-glycoprotein (Pgp, MDR1 or ABCB1) took us

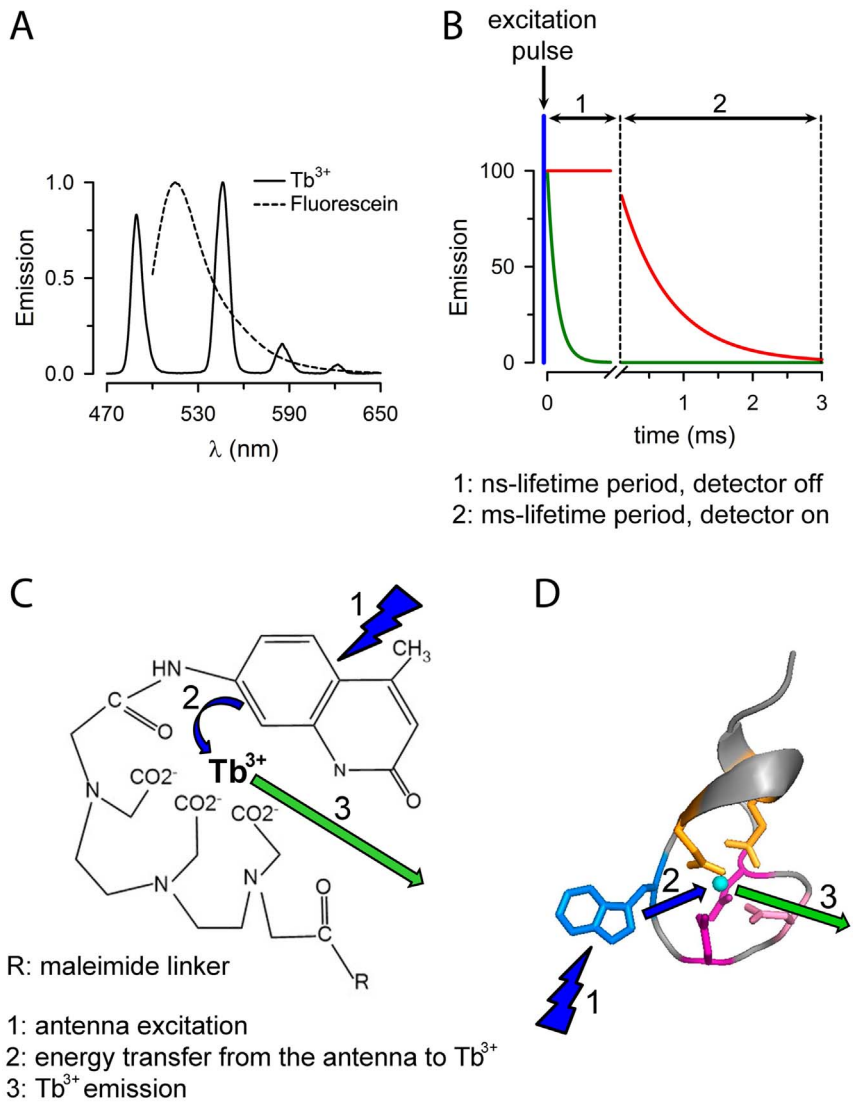

Fig. 2. Luminescence resonance energy transfer (LRET). A. Emission spectra of the Tb^{3+} chelate LRET donor and fluorescein. The Tb^{3+} sharp emission with dark regions between peaks contrasts with the broad emission spectra of fluorophores such as fluorescein. B. Use of gated emission in LRET. Representative of typical LRET gated emission (red, period 2) after a delay of microseconds (period 1) that follows a short 337 nm ns-excitation pulse. Emissions that decay with ns lifetimes (during period 1) are depicted in green. C. Luminescent lanthanide probe with separate chelator and antenna. Example of a polyaminocarboxylate-carbostyril probe consisting of a DTPA chelate and cs124 antenna. R represents the maleimide group. D. Genetically-encoded lanthanide binding tag (LBT) where chelator and antenna are part of the same structure. Ribbon representation of Tb^{3+}-LBT complex with the Tb^{3+} (cyan sphere) coordinated by ligands of two Asp (magenta sticks), two Glu (orange sticks), a Asn (pink sticks) and the backbone carbonyl group a Trp (blue), which also serves as antenna. Energy from the carbostyril (panel C) or Trp (panel D) excited by a short pulse (1) is transferred to the Tb^{3+} (2), which produces long lifetime emission (3).

a lot more effort because we had to do it in stages by directed evolution using a powerful drug resistance screen [36].

A number of thiol-reactive luminescent lanthanide chelates suitable as LRET donors are commercially available or have been synthesized [26,27,30,37,38], but we generally use the Tb^{3+} chelate DTPA-cs124-EMCH (Fig. 2C) [28–30,35,39–41]. It has a maleimide for covalent reaction with Cys thiols, a carbostyril antenna chromophore that absorbs well at 335 nm (cs124; 7-amino-4-methyl-2(1H)-quinolinone; good for excitation with a nitrogen laser), and the high-affinity diethylenetriaminepentaacetic acid (DTPA) chelator. The antenna absorbs the excitation light (Fig. 2C, step 1) and transfers it to the Tb^{3+} with high efficiency (Fig. 2C, step 2), whereas the chelator shields the Tb^{3+} from the broadening effects of the water, keeping the Tb^{3+} spectral peaks sharp. This compound is water soluble and displays a lifetime of ~2 ms, high-quantum yields, large Stokes shifts, and emission spectra with sharp peaks [30]. Even though the size of the probe places the Tb^{3+} away from the Cys α carbon, this seems to be a minor problem because the donor-acceptor distances determined in several systems are very close to those estimated from crystal structures [28,35,39,42,43]. This is likely the result of positioning of the probes on the outside of the structure, away from other areas, and the unpolarized long lifetime of the LRET sensitized emission that allows the probes to sample all orientations, centered close to the α carbon. If needed, the position of the probes can be modeled based on the protein structure and LRET parameters [44–46].

One positioning approach alternative to the chemical labeling is the use of genetically-encoded lanthanide-binding sequences [31–34,47,48]. These are sequences derived of the EF hand motifs of Ca^{2+}-binding proteins, which display high affinity for lanthanides [31,32] and have been successfully introduced in proteins for LRET studies [31,33,34]. These tags include acidic coordination residues and a Trp residue that functions as antenna (Fig. 2D). Since the structure of the lanthanide binding tags and the atomic distances within the tag complex are known, their use could allow for more precise predictions of the location and orientation of the donor. In principle, lanthanide binding tags can be used in combination with tetracysteine tags that react with fluorescent biarsenicals acceptors [49,50]. Lanthanide binding tags minimize the need to work with purified proteins. In fact, combining the use of tags or specific binders has allowed for measurements of atomic distances of MPs such as the Na,K-ATPase and ion channels in intact cells [33,34,47].

3.3. LRET data analysis

The relevant long-lifetime emissions used for LRET calculations are those from the luminescent lanthanide donor and the sensitized emission of the acceptor fluorophore [26]. The distance between the donor and acceptor can be calculated from:

$$R = R_0 \, (E^{-1} - 1)^{1/6}, \quad (1)$$

where E is the efficiency of energy transfer calculated as:

$$E = 1 - \tau_{DA}/\tau_D, \quad (2)$$

R_0 is the Förster distance (distance at which $E = 0.5$), and τ_D and τ_{DA} are the lifetimes of the donor in the absence and presence of the acceptor, respectively. In LRET, the sensitized acceptor emission is essentially equal to τ_{DA} (see Section 3.1). R_0 is calculated from the spectral properties of donor and acceptor according to:

$$R_0 = 0.21 \, (J \, q_D \, n^{-4} \, k^2)^{1/6} \, (\text{in Å}), \quad (3)$$

where J is the normalized spectral overlap of the donor emission and acceptor absorption, q_D is the donor quantum yield in the absence of acceptor, n is the refractive index, and κ^2 is a geometric factor related to the relative orientation of the transition dipoles of the donor and acceptor and their relative orientation in space.

The orientation factor κ^2 is related to the angle between the donor and acceptor transition dipole moments and is a source of uncertainty in FRET measurements. The extreme values of κ^2 are zero if all angles are 90°, and 4 if all angles are 0°. Its value equals 2/3 if the donor and acceptor rotate rapidly and completely during the lifetime of the donor excited state. Constraints can be imposed by measuring the polarization of donor and acceptor emissions to reduce the uncertainty in κ^2. Considering the unpolarized emission of Tb^{3+} chelates and that the acceptor will very likely rotate during the long donor lifetime, errors in distances calculated from LRET due κ^2 are negligible. This makes distance calculations based on LRET data generally more accurate than those based on FRET data.

In our hands, sensitized emission lifetimes in ABC exporters are few and can be determined easily and accurately by fitting the LRET decays to a multi-exponential function, with the fitting quality assessed from the random residual distribution, which should not show structure and have a chi-squared value near unity. Two key parameters can be obtained from the multi-exponential fitting of the donor only and sensitized acceptor emission decays: the intensity of each component at time = zero (pre-exponential term), and the decay lifetime. The latter can be used to calculate E (Eq. (1)) and donor-acceptor distances (Eq. (2)). The percentage of donor-acceptor pairs showing a specific distance can be calculated from the fractional intensity contribution of each distance component divided by the rate of energy transfer ($k = 1 / \tau_{DA} - 1 / \tau_D$) [35,39].

In addition to the multi-exponential fitting that unveils predominant donor-acceptor pair distances, we routinely use an exponential series method designed to recover lifetime distributions without a priori assumptions about the distribution shape [39,51,52]. For this, we analyze the LRET sensitized emission decays using a series of 200 exponentials with variable pre-exponentials and fixed, logarithmically-spaced lifetimes. The lifetime distributions can then be converted to distance distributions. Since the analysis does not have assumptions about the distributions shapes, it can be used to discriminate between discrete and continuous distance distributions.

3.4. Applications of LRET

The applications of LRET are many and include its use in biochemical assays, measurements of protein-protein and protein-DNA interactions, determination of the oligomeric composition of proteins, and assessment of conformational changes of DNA and proteins [26]. The use of LRET in high-throughput screening assays is particularly important. Its widespread use is based on the facts that the assays are not radioactive and do not require separation of products or washes, that LRET is highly sensitive, and that E can be measured over relatively long distances. The high sensitivity and signal-to-noise ratio of LRET is particularly appealing because it allows analysis of poorly-labeled samples in complex preparations (*e.g.*, cell lysates) and can be detected at sub-nM concentrations, reducing the use of expensive reagents. Also, since LRET occurs over a fairly long distance range (10–100 Å), it is possible to use the same lanthanide-labeled "large" reagents (*e.g.*, antibodies, streptavidin) for different assays (*e.g.*, labeled streptavidin for assays of a variety of biotinylated binders).

Relevant to focus of this review, LRET has been used in a number of membrane protein studies for diverse purposes, including determinations of conformational changes [29,33,34,42–44,47,53–60]. Here, we will discuss the use of LRET to follow ABC proteins conformational changes in Sections 4 and 5.

4. ABC proteins superfamily

ABC proteins comprise one of the largest protein families, with members in all kingdoms of life [61,62]. ABC importers are found predominantly in bacteria and archaea, whereas most eukaryote ABC proteins are exporters [61,63,64]. The human ABC protein family includes 49 members, which are divided into 7 sub-families based on sequence similarities [61,62,65]. Except for the ABCE and ABCF members, which comprise 4 soluble regulatory proteins, human ABC proteins are multispanning transmembrane proteins. The majority are exporter pumps localized to the plasma membrane, which contribute to the reduction of intracellular concentration of their substrates. The ABCC subfamily has a few exceptions of members that do not work as exporter pumps, the Cl^- channel CFTR (ABCC7; cystic fibrosis transmembrane conductance regulator), and the regulatory subunits of K_{ATP} channels SUR1 and SUR2 (ABCC8 and ABCC9, respectively; sulfonylurea receptors) [65–67]. The substrates of ABC exporters are varied and include endogenous molecules, environmental contaminants and drugs used for the treatment of human diseases [62,65,68]. These pumps are also integral parts of the placental, blood-brain and blood-testis barriers [69,70]. Therefore, ABC exporters play important roles in human physiology, pathophysiology, blood-tissue barriers and drug pharmacokinetics. ABC exporters such as Pgp transport cytotoxic agents used to treat cancer and have been associated with cancer multidrug resistance [62,65,71].

4.1. ABC exporters

The basic structural/functional unit of human ABC exporters consists of two halves, each containing a helical transmembrane domain (TMD), generally formed by six α helices, and a nucleotide binding domain (NBD) (Fig. 3) [61–63,65]. In Pgp and many other ABC exporters the TMD1-NBD1-TMD2-NBD2 structure is part of a single polypeptide, with intracellular N- and C-terminal ends (Fig. 3A). Several exporters have an additional N-terminal domain (TMD0) formed by several transmembrane α helices. The TMD0s of MRP1 and other ABCC proteins have 5 transmembrane helices linked to the basic core structure by the L0 loop (Fig. 3B) [65,66,68]. The transporter associated with antigen processing (TAP1/TAP2), a heterodimer formed by TAP1 (ABCB2) and TAP2 (ABCB3), has a 4-transmembrane helix TMD0 that functions as a transmembrane interaction hub for the assembly of the peptide loading complex (Fig. 3C) [67].

The hydrophobic TMDs vary within ABC exporters, whereas the NBDs are structurally conserved. Since the TMDs form part of the pathway for substrate transport across the membrane, the diversity of TMDs is consistent with the need for binding sites and transport pathways for very different substrates. In contrast, the conserved NBDs bind and hydrolyze nucleotide triphosphates, a common function that provides the energy for transmembrane transport. Thus, the common nucleotide binding and hydrolysis functions of ABC proteins have structurally-conserved NBDs at their core. The NBDs contain several conserved sequences that are important for ATP binding and hydrolysis, which include the Walker A motif (motif A or P-loop), the Walker B motif (motif B), the signature sequence (motif C), the A-loop, the H-loop (H-switch), the Q-loop and the D-loop (Fig. 4A). Upon ATP binding, the

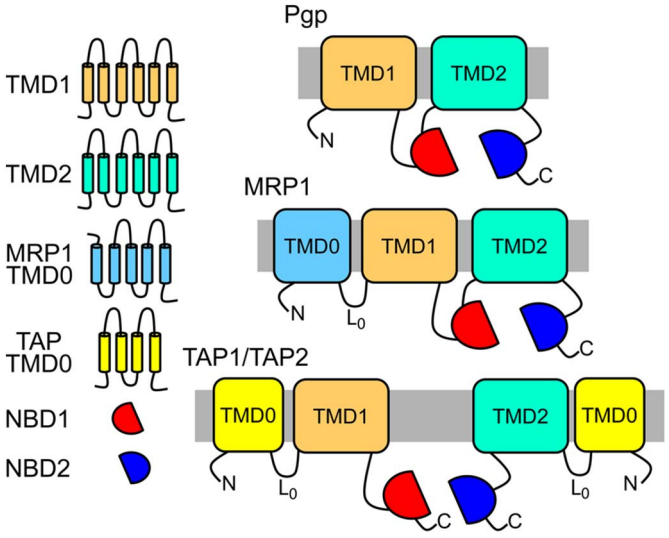

Fig. 3. Domain structure of three human ABC exporters. Schematic representation of P-glycoprotein (Pgp), multidrug resistance protein 1 (MRP1) and the transporter associated with antigen processing (TAP; TAP1/TAP2). Transmembrane α-helices are depicted as cylinders. TMD: multispanning transmembrane domain. NBD: nucleotide binding domain. L_0: linker or lasso domain.

NBDs dimerize in a head-to-tail orientation, with two ATP molecules bound at the NBD-NBD interface (Fig. 4B). In the nucleotide-bound NBD dimer, each of the two nucleotide-binding sites (NBSs) is formed by the Walker A motif, Walker B motif, A-loop, H-loop and Q-loop of one NBD, and the D-loop and signature motif of the other NBD (Fig. 4A) [72,73]. The Walker A motif is involved in binding of nucleotide phosphates and the Walker B, which ends with the catalytic Glu, is involved in Mg^{2+} and water coordination, and together with the D-loop, it positions and activates the attacking water for ATP hydrolysis [72,73]. The D-loop is also important for NBD dimerization since upon ATP binding the D-loop Asp of each NBD forms hydrogen bonds and an electrostatic network with the H-loop and Walker A motif of the other NBD, and the two D-loop backbones interact with each other [72,74,75]. The A-loop contains a conserved aromatic residue that interacts with the purine or pyrimidine rings of nucleotides and it is important for nucleotide binding (Fig. 4A) [72]. The general view is that ATP hydrolysis by the NBDs is catalyzed *via* a general base mechanism where the carboxylate of the end of the Walker B motif polarizes the hydrolytic water that attacks the γ-phosphate of ATP [72]. However, it has also been proposed that the Walker B Glu is part of a complex that stabilizes the transition state rather than being a catalytic base [76].

The functional unit of most ABC exporters has two identical (*e.g.*, MsbA) or very similar NBDs (*e.g.*, Pgp), with two NBSs that can hydrolyze ATP [63]. However, in a few human exporters only one of the NBSs is catalytically competent [63]. For example, an Asp replaces the catalytic Glu in several ABCC proteins, including CFTR and MRP1, and the side chain of this Asp may not be long enough to interact with the hydrolytic water [63,77,78]. In some proteins such as MRP1, the NBD2 signature sequence also deviates from the LSGGQ consensus sequence [77]. Even though the two NBDs of proteins such as Pgp and its bacterial homologue MsbA are very similar, there is evidence for asymmetry in the structure and function of the NBD dimer [79–82]. A Pgp model based on biochemical and structural data proposes that ATP hydrolysis occurs at one site, with alternating site catalysis where only one of the two ATP molecules is bound tightly and committed to hydrolysis ("trapped") [79,83]. It is still unclear how this binding and hydrolysis of ATP in the NBDs is translated into substrate transport by the TMDs.

4.2. Molecular mechanism of ABC exporters

In spite of decades of studies, our understanding of the mechanism of ABC exporters is very limited and there is no agreement on the molecular mechanism of operation. Except for the case of the lipid-linked oligosaccharide flippase PglK, for which transport seems to occur only through outward-facing conformations [64], it is thought that ABC exporters operate by alternating the access to their transmembrane central cavity between both sides of the membrane [64]. The general view is that formation of the ATP-bound NBD dimer drives rearrangements in the TMDs that result in the transition from an inward-facing, open conformation (dissociated NBDs or loosely-associated NBDs) to an outward-facing, closed conformation (tight ATP-bound NBD dimer) (Fig. 5A). In plasma-membrane ABC exporters such as Pgp, in the inward-facing conformation the binding pocket would be accessible to the inner leaflet/cytoplasm, whereas in the outward-facing conformation the pocket accessibility will switch to the extracellular side. Bound transport substrates will then be released from this outward-facing conformation into the external medium. The NBD dimerization elicited by ATP binding would provide the power stroke, and the NBD dissociation or dimer opening that follows ATP hydrolysis would reset the exporter for the next cycle.

A number of models have been proposed to explain the conformational changes that take place during the ATP hydrolysis cycle in the NBDs. They can be generally divided into: 1) monomer/dimer models, where dissociation of the NBD dimers follows ATP hydrolysis [72,84–88], and 2) constant-contact models, where the NBDs remain in contact during the hydrolysis cycle [89,90]. A schematic representation of these general models is presented in Fig. 5C: one proposing complete NBDs dissociation (monomer-dimer models) and the other continuous contact between the NBDs (constant-contact models). The crystal structures of Pgp and MsbA (obtained in the absence of lipids), and DEER spectroscopy studies, support the monomer/dimer models view

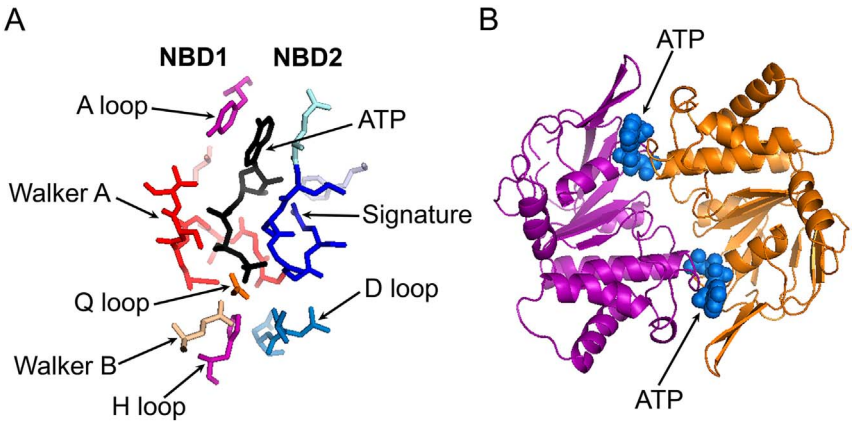

Fig. 4. Structure of the NBD dimer. A. View of a nucleotide-binding site. Stick representation showing the ATP (black) and several conserved sequences. Other residues were removed to make viewing easier. B. Ribbon representation of the ATP-bound MJ0796 dimer. Monomers are displayed in purple and orange, and ATP molecules in blue. Based on the structure of the catalytically-inactive MJ0796-E171Q mutant PDB 1L2T.

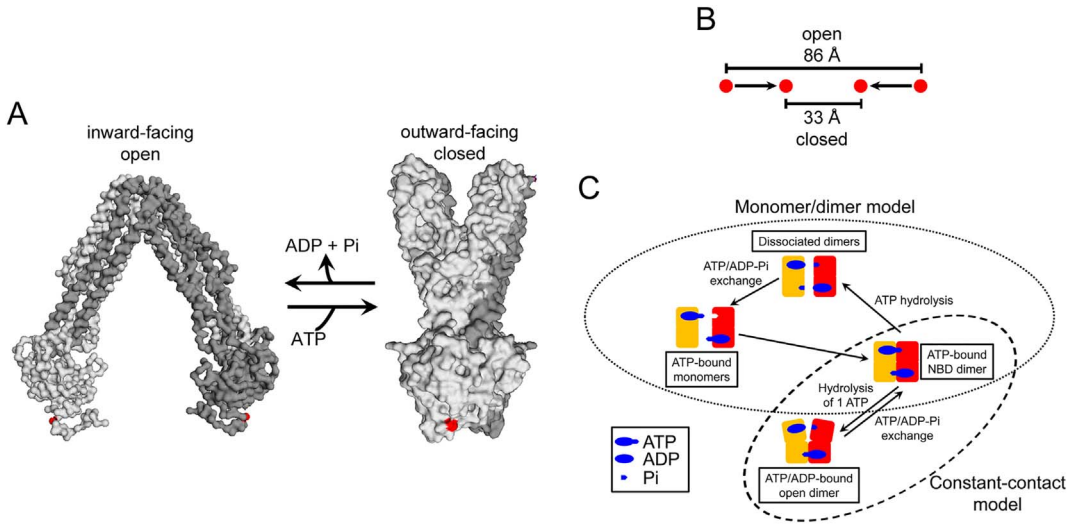

Fig. 5. NBD-NBD interactions during the ABC protein hydrolysis cycle. A. Model of ABC exporter operation based on MsbA crystal structures. Monomers are represented in different tones of gray. The residue at position 561, used for LRET experiments (T561C mutant) is labeled red. Based on PDB 3B5W (open conformation) and PDB 3B60 (closed conformation). B. Schematic representation showing the αC-αC distances in the open and closed conformations. C. Models of NBD interactions during the catalytic cycle. Panel B has been modified from reference [34], with permission from the American Society for Biochemistry and Molecular Biology.

that large conformational changes on the NBDs side (of ~30 to > 60 Å) take place when the exporters switch between the inward- and outward-facing conformations (Fig. 5A and B) [91–95]. However, the existence of such large conformational changes have been put in doubt by the nucleotide-bound, outward-facing structure of the bacterial homodimer exporter Sav1866, where interactions between the two subunits are expected to make a significant separation of the NBDs difficult at best [89]. The Sav1866 structure agrees with results from electron microscopy structures of Pgp in a lipid bilayer [96] and with our recent spectroscopy studies in MsbA [35,39], which point to close proximity of the NBDs in the nucleotide- and substrate-free (apo) state. This notion is consistent with Cys cross-linking studies showing that the C-terminal ends of the two Pgp NBDs do not need to separate significantly during the drug-stimulated catalytic cycle [97,98]. These data suggest that the NBDs remain in contact, or very close to each other, during the hydrolysis cycle, and that large conformational changes on the NBDs side might not be physiological. However, differences between the modes of operation of Sav1866 and other exporters such as Pgp are possible. For example, in contrast to Sav1866 [89], Pgp seems to prefer the inward-facing conformation, probably because of its increased substrate binding pocket hydrophobicity and charge density of the NBDs interface [99,100].

Discrimination between the two sets of models in Fig. 5C can be directly addressed using steady-state LRET and LRET kinetics. Comparison of steady-state distances between the NBDs in the nucleotide-free monomer state, ATP-bound dimer state and during hydrolysis can provide information needed to distinguish between monomer/dimer and constant-contact models. But LRET can also be used to study the kinetics of the conformational changes, an issue frequently neglected in structural-functional studies of ABC proteins. Experiments under steady-state conditions, where the NBDs are “locked” in specific states (*e.g.*, nucleotide-free, ATP-bound) can determine that it is possible to obtain a given conformation under the experimental conditions used, but it does not provide information on the relevance of that conformation in the catalytic cycle. Measuring the kinetics of the conformational changes and correlating those changes with the function (*e.g.*, rate of ATP hydrolysis) can provide essential information for a complete understanding of the catalytic cycle. For example, the finding of dissociated NBDs by itself just indicates that the NBDs can separate during the hydrolysis cycle. However, if the rate of NBDs dissociation is much slower than the rate of hydrolysis, it can be concluded that the dissociation is a rare event that occurs only after many hydrolysis cycles. Therefore, LRET represents a powerful technique for the study of ABC transporters and other MPs.

5. Application of LRET for the study of isolated nucleotide-binding domains

5.1. *Methanocaldococcus jannaschii MJ0796 as a prototypical ABC NBD*

Although understanding of the NBD-NBD interactions in ABC proteins requires studies in full-length proteins, isolated NBDs (expressed without their TMDs) constitute a much simpler system, where basic details of the structure and function can be explored. However, attempts to study isolated NBDs from eukaryote ABC proteins, and even prokaryote ones, have been disappointing, with eukaryote NBDs unable to dimerize efficiently in response to ATP binding, or prokaryote NBDs able to dimerize only after mutations that render their ATPase activity very low. MJ0796 from the thermophile *M. jannaschii* is a notable exception. MJ0796 is a homolog of the *E. coli* LolD, the NBD of the LolCDE transport system that mediates the translocation of lipoproteins from the inner membrane to the outer membrane [101]. MJ0796 has been used extensively for biochemical, biophysical and structural studies [28,40,41,72,102–105], and the crystal structure of the ATP-bound form was the first for an NBD dimer of an ABC transporter [72,105]. MJ0796 is a simple system because the dimer is formed by two identical NBDs. Additional advantages for spectroscopic studies are that MJ0796 has no native Trp residues and only two Cys. This simplifies the mutagenesis needed to introduce Trp residues that can be used as spectroscopy environment probes, and the creation of single Cys mutants for chemical attachment of LRET probes.

5.2. *Tryptophan fluorescence spectroscopy to assess NBD conformational changes*

Trp fluorescence is a classical spectroscopic technique that has been widely used to study conformational changes in proteins because Trp emission is highly sensitive to its environment. Trp residues have been introduced into specific positions of the otherwise Trp-less MJ0796, generating two mutants, Tyr11Trp and Gly174Trp, which are catalytically active, and have been used to follow ATP-dependent dimerization by the quenching of the Trp emission [72,104,105]. The Trp174 is located at the center of the NBDs dimer interface, and the ATPase activity of this mutant is similar to that of wild-type MJ0796 [104,105]. The

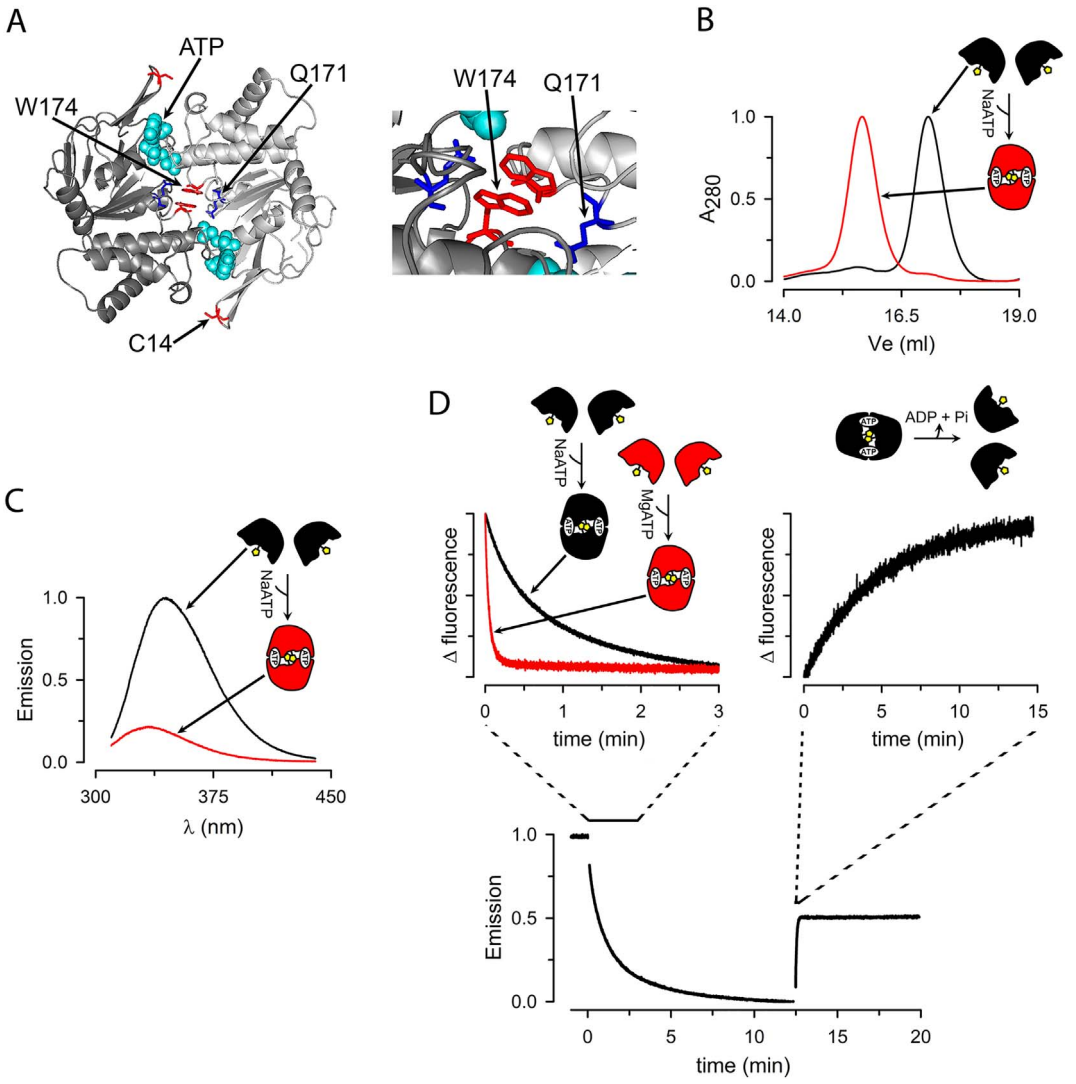

Fig. 6. NBD association/dissociation. A. Structure of the MJI NBD dimer. Top: ribbon representation of the ATP-bound MJI dimer. Monomers are displayed in different tones of gray and ATP molecules in cyan. Trp174 (G174W mutation), Q171 (E171Q mutation) and Cys14 (G14C mutation) are also shown (sticks). Bottom: Expanded view of the center of the dimer interface showing the two Trp174 residues (pink sticks) in a parallel π stacking interaction. Based on PDB 3TIF. B. Dimerization in response to ATP (> 20 folds the EC_{50}) increases the hydrodynamic radius as determined by size-exclusion chromatography. A_{280}: absorbance measured at 280 nm, normalized to the peak value. C. Dimerization in response to ATP. ATP (> 20 folds the EC_{50}) produces Trp emission quenching. D. Time course of the monomer/dimer equilibrium following ATP binding and hydrolysis. The final concentrations of ATP and Mg^{2+} were 2 and 10 mM, respectively. Bottom: complete time course. Top left: time course of MJ Trp-174 fluorescence quenching by NaATP (black) and MgATP (red) after rapid mixing in a stopped-flow device. Top right: time course of the Trp-174 fluorescence increase elicited by Mg-dependent hydrolysis after rapid mixing. Panels B–D have been modified from reference [101], with permission from the American Society for Biochemistry and Molecular Biology.

location of the Trp residue at the dimer interface was confirmed by X-ray crystallography of a nucleotide-bound Gly174Trp mutant where the catalytic carboxylate Glu171 was substituted with Gln. This mutant (MJ0796-E171Q/G174W) has essentially no ATPase activity and forms very stable dimers, suitable for crystallization, in the presence of ATP. The structure of the dimer in Fig. 6A [105] shows the Trp174 residues of each NBD in a π stacking (**1p**, parallel configuration) near the center of the dimer interface (Fig. 6A). This short distance between the Trp indole rings (3.0–3.5 Å) in the dimeric NBDs can account for the quenching of Trp emission upon dimerization, as discussed below; Trp-Trp FRET homotransfer ($R_0 \sim 5$–15 Å) [106] surely plays an important role in the quenching, but other mechanisms (*e.g.*, static quenching) are also likely to contribute [107].

The Trp-Trp aromatic interactions, dominated by van der Waals forces, could add as much as 3 kcal/mol to the dimer binding energy [108], which could account for the increased dimer stability that allows for the observable presence of nucleotide-bound MJ0796-G174W active dimers in solution by size-exclusion chromatography (SEC), whereas such dimers had been observed before only for catalytically inactive NBDs [87]. The complete formation of dimers at a saturating concentration of ATP (and disappearance of monomers) [105], indicates that essentially all NBDs can form ATP-bound dimers (Fig. 6B). Such dimerization of active NBDs in solution was also observed by quenching of the Trp174 emission after addition of ATP (Fig. 6C) [105]. The high fluorescence of monomeric NBDs decreases as dimers are formed, largely as a result of the Trp-Trp π stacking. Fig. 6C also shows that, in addition to the quenching, in the NBD dimers the Trp174 emission peak experiences a blue shift of ~10 nm [105], consistent with the decreased solvent accessibility of the Trp residues in the dimer [105].

The quenching of Trp174 emission provides a way to follow conformational changes of the NBDs in real time. For example, Fig. 6D (top inset) shows fast dimerization (quenching) when NBDs are mixed in a stopped-flow chamber with their physiological substrate, MgATP (red), whereas the dimerization in response to NaATP, also at a saturating concentration is slower (black) [105]. The faster dimerization by MgATP *vs.* NaATP is likely the result of Mg^{2+} coordination at the active

site and electrostatics at the dimer interface [72]. Interestingly, Fig. 6D (bottom inset) also shows a partial recovery of the Trp174 emission with the transition from NaATP-bound dimers to a continuous hydrolysis state after Mg^{2+} is added to initiate hydrolysis. The fluorescence value during ATP hydrolysis is approximately halfway between those corresponding to the monomers and dimers [105]. As expected, this effect is not observed in the catalytically-inactive MJ0796-E171Q/G174W, where the protein stays as ATP-bound dimers in the presence of MgATP [28,105]. It is tempting to conclude that the partial recovery of Trp emission during hydrolysis is the result of dissociation of the MJ0796-G174W dimers, and that the rate of Trp emission recovery, which can be measured by mixing ATP-bound dimers with $MgCl_2$ in a stopped-flow device (Fig. 6D, right side inset), is related to the dimers' dissociation rate. This conclusion will be consistent with the dissociation of ATP-bound MJ0796-G174W dimers observed by SEC in response to Mg^{2+} [105]. However, this interpretation is not necessarily correct since this partial Trp fluorescence increase cannot only be the result of dissociation of the dimers, with re-association to reach a new equilibrium with less dimers, but also the result of an opening of the dimers that breaks the Trp-Trp π stacking interaction, without complete dissociation of the NBDs. LRET is an ideal technique to determine whether the NBDs actually separate during hydrolysis and to determine the rate of dimer dissociation.

5.3. Following NBDs association/dissociation in real time by LRET

For the LRET experiments the native Cys of MJ0796-G174W and MJ0796-E171Q/G174W, Cys53 and Cys128 were replaced with Gly and Ile, the residues at the equivalent positions in MJ1267, a related *M. jannaschii* NBD [28]. The resulting Cys-less NBDs have biochemical and functional properties very similar to those of the parent NBDs, even after labeling with the LRET probes [28]. Then, a single-Cys was introduced for labeling with the LRET probes at position 14 to produce MJ0796-G14C/G174W and MJ0796-G14C/E171Q/G174W, which we referred to as MJ and MJI (catalytically-inactive MJ), respectively. Position 14 was selected because it is on the NBD surface (away from the active site in the dimer interface), exposed to the aqueous solvent (suitable for labeling), and the Cys14-Cys14 distance in the dimer, estimated from the MJI crystal structure, is ~50 Å [28,105], quite compatible with common LRET donor-acceptor pairs such as Tb^{3+}-fluorescein (R_0 = 46 Å) (Fig. 6A). Therefore, these mutant NBDs containing a single Trp at position 174, and a single Cys at position 14, can be used as a model system to study the dimerization process by traditional Trp fluorescence and by LRET.

As shown in Fig. 7A (black), similarly to what was observed for the MJ0796-G174W mutant with native Cys, addition of a saturating concentration of NaATP produced a slow Trp quenching that is the result of ATP-induced dimerization. Once all NBDs are ATP-bound dimers, addition of Mg^{2+} starts ATP hydrolysis, with a partial recovery of the Trp emission. Fig. 7A also shows equivalent LRET experiments performed on the Cys14 NBDs labeled separately with donor and acceptor probes and then mixed in equimolar proportion (red). The LRET intensity looks like a mirror image of the Trp emission quenching (black), as expected from the increase in energy transfer when the NBDs are closer (opposite to the increase Trp quenching upon dimerization) [28,105]. Addition of NaATP increases LRET intensity, and during hydrolysis the LRET signal decreases to a value close to that halfway between that in the nucleotide-free monomers and the ATP-bound dimers [28,105]. However, there is an important difference between Trp quenching and LRET spectroscopy. The analysis of LRET intensity decays (this is, the time that the sensitized emission of acceptor takes to decay after a single excitation pulse) can provide information on the Cys14-Cys14 distance from the analysis of LRET decay lifetimes. As discussed in Section 3, lifetimes can be used to calculate donor-acceptor distances. Fig. 7B shows that the low intensity and slow decay in the nucleotide-free state (NBD monomers, black), is replaced by a high intensity and faster decay in the presence of NaATP (ATP-bound dimers, red). At NBD concentrations in the 0.5–1 μM range, and in absence of ATP, the average distance between NBDs is > 1100 Å and LRET is negligible, but upon NaATP-induced dimerization LRET increases dramatically, as expected from the fact that essentially all NBDs are present as dimers [28,41]. When LRET decays are visualized in a semi log scale, the single straight line indicates the presence of a single donor-acceptor distance (Fig. 7C). Calculations indicate that the distance is ≫100 Å in the nucleotide-free state (as expected from momoneric NBDs), and ~50 Å in the ATP-bound state and during ATP hydrolysis. It follows that if the NBD dimers dissociate, the decrease in LRET during hydrolysis will be the result of a reduced number of dimers, and then the donor-acceptor distance will remain unchanged; the lower intensity will be the result of a reduced number of dimers with the same Cys14-Cys14 distance as in the ATP-bound state. In contrast, if the dimers open without dissociation, the decrease in intensity during hydrolysis will result from an increase in the donor-acceptor distance, with slower rate of LRET intensity decay. A combination of both phenomena will produce a mix, and the decay will not follow a single-exponential function. The results in Fig. 7C clearly show that the rates of sensitized emission LRET intensity decays in the ATP-bound state and during hydrolysis are the same (two parallel straight lines), indicating that the number of dimers is reduced during ATP hydrolysis, and that there is no new distance, as will occur with a partial opening of the dimers.

5.4. Determining the number of ATPs hydrolyzed per NBD dimer dissociation

Considering that the one of the NBSs of proteins such as CFTR and MRP1 is not catalytically active, it is possible that the molecular interactions between the NBDs in such ABC proteins are different from those in proteins with two catalytically-active NBSs such as MsbA and Pgp. This issue is related to a general question in the field that is: Are both ATPs bound to the NBD dimer hydrolyzed during a hydrolysis cycle or just 1?

Computational simulations suggest that ATP hydrolysis at one site is sufficient to induce opening of the NBD dimer [109,110], but because of the absence of direct measurements a number of molecular models have been proposed [72,79,87–89,102,111,112]. These include various models where one or two ATPs are hydrolyzed *per* cycle, including sequential hydrolysis of both ATPs before NBDs dissociation [87], and alternate hydrolysis between the two NBSs with one hydrolysis *per* cycle [79,83]. LRET has proven useful to address this issue [41]. Fig. 7D shows a real-time measurement of the association and dissociation of NBDs that have two NBSs, but only one hydrolytic site. For this experiment, the active MJ was labeled with the maleimide Tb^{3+} chelate as donor, and the inactive MJI with fluorescein maleimide as acceptor. Upon mixing the NBDs in equimolar proportion LRET is negligible in the absence of ATP because the NBDs are monomers, too far away from each other for efficient LRET. However, upon addition of a saturating concentration of NaATP LRET increases because of formation of MJ/MJI heterodimers (Tb^{3+}/fluorescein). MJ/MJI heterodimers (visible by LRET) are expected to be ~50% of the dimers for a random mix, with the remaining being homodimers (essentially invisible by LRET): ~25% of catalytically-active MJ/MJ homodimers (Tb^{3+}/Tb^{3+}) and ~25% of catalytically-inactive MJI/MJI homodimers (fluorescein/fluorescein). Thus, only the heterodimers that have two NBSs and one functional ATP hydrolysis site are followed by LRET in real time. Addition of Mg^{2+} to initiate and maintain hydrolysis produces a decrease in LRET intensity. This result indicates that the MJ/MJI heterodimers dissociate following ATP hydrolysis, but since only one NBS is catalytically active, this dissociation must occur after hydrolysis of a single ATP. The experiment in Fig. 7E illustrates a typical example where the rate of MJ/MJI heterodimer dissociation is directly compared with that of MJ/MJ homodimers. Basically, ATP-bound dimers were rapidly mixed with $MgCl_2$ and a large excess of unlabeled MJ in a stopped-flow device.

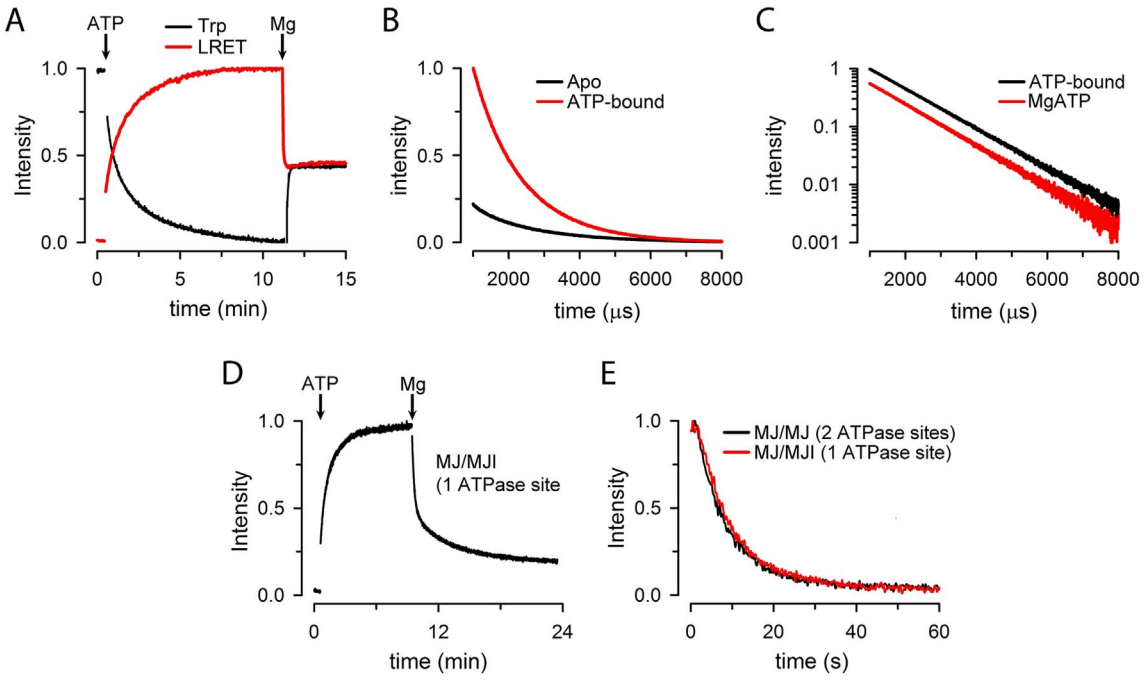

Fig. 7. NBD association/dissociation followed by LRET. A. Time course of MJ NBD association/dissociation monitored by LRET and Trp quenching. ATP and $MgCl_2$ were used at 2 and 10 mM, respectively (saturating concentrations). MJs labeled with Tb^{3+} chelate or fluorescein were mixed for the LRET experiments. For the Trp quenching experiments the MJs were not labeled. Sensitized fluorescein emission was measured at 520 nm and the signals were normalized to the total change. B. Effect of ATP on the sensitized fluorescein emission decay from MJ. Black (No ATP) and red (ATP). Intensities were normalized to the ATP intensity at 200 μs. C. Effect of MgATP on the MJ sensitized fluorescein emission decay. Semi-log plot of the ATP (black) and MgATP (red) decays. D. Changes in sensitized fluorescein emission from MJ/MJI heterodimers during the hydrolysis cycle. These heterodimers have two nucleotide binding sites, but only one can hydrolyze ATP. Tb^{3+}-labeled MJ and fluorescein-labeled MJI were mixed in a 1:1 molar ratio. E. Time course of the dissociation of MJ homodimers and MJ/MJI heterodimers. Dissociation of ATP-bound dimers labeled with LRET probes followed by rapid mixing in a stopped-flow cell with $MgCl_2$ to start ATP hydrolysis. Panels A–E have been modified from references [27,40], with permission from the American Society for Biochemistry and Molecular Biology.

When the dimers dissociate following hydrolysis, they re-associate largely with unlabeled MJ (no LRET), and the rate of decrease in LRET is equivalent to the rate of dimer dissociation. Once again, with LRET it is possible to follow the behaviour of the molecules of interest within a complex mix. The results in Fig. 7E clearly indicate that the rates of dissociation of MJ/MJ (two hydrolysis sites) and MJ/MJI (one hydrolysis site) are identical. Moreover, the MJ/MJ and MJ/MJI dissociation rates and the rate of ATP hydrolysis under the same experimental conditions are virtually the same [41]. The equality between the rates of hydrolysis and dissociation of MJ homodimers indicates hydrolysis of only one of the bound ATPs. Overall the results indicate that a single hydrolysis event can drive NBD dimer dissociation, even when the NBD dimer is formed by two identical NBDs. These results suggest that the molecular mechanism is not necessarily different for ABC proteins with one (MRP1) and two (Pgp) hydrolysis sites.

5.5. The role of the two ATP binding sites in NBD dimer formation

One obvious question that follows the observation that only one hydrolysis event is needed to dissociate ATP-bound NBD dimers is why do ABC proteins have two NBSs. This can also be easily answered using LRET in isolated NBDs [40]. In this case, MJ/MJ mutant heterodimers can be engineered to control the average occupation of the NBSs. When they associate with MJ, the resulting NBD dimers will form one “normal” NBS and one low affinity NBS [40]. Lys44 is a conserved residue in the Walker A motif that participates in ATP binding through interactions with the nucleotide phosphates, and its mutation to Ala decreases the affinity for ATP [72,84]. The EC_{50} values for NaATP- and MgATP-induced dimerization of MJ are ~50 and < 5 μM, respectively. As a result, MJ homodimers are readily formed in 500 μM NaATP or ~10 μM MgATP [40]. The EC_{50} values for NaATP- and MgATP-induced dimerization of the MJ-K44A mutant are ≫500 and ~70 μM, respectively. As a result, MJ-K44A homodimers (two low-affinity NBSs) are not formed in 500 μM NaATP or 10 μM MgATP, but are produced in 500 μM MgATP [40]. The study of heterodimers formed by one MJ (Tb^{3+}-labeled) and one MJ-K44 (fluorescein-labeled) as a function of the number of NBSs occupied by ATP, indicates that dimers are not formed under conditions where only one of the NBSs is occupied (low ATP concentration; 500 μM NaATP or 10 μM MgATP), but form when both NBSs are occupied (500 μM MgATP). Hence, it appears that occupation of the two NBSs of ABC proteins is essential to produce an ATP-sandwich dimer of sufficient stability to allow for ATP hydrolysis at one of the NBSs.

All together this information illustrates LRET as a powerful technique that can help answer many basic questions about the molecular mechanism of MPs, which can be applied to the study of relatively simple but important domains, such as the conserved NBDs of ABC transporters, or can be used for the study of full-length MPs, in conditions that approach the physiological environment of these proteins, as is discussed below.

6. Application of LRET to a full-length ABC exporter

6.1. MsbA as an ABC exporter model

Although many ABC transporters have been studied by different approaches, there is not a general consensus to explain how they function at the molecular level. Many discrepancies between the results that serve as bases for the alternative models of the molecular mechanisms of ABC exporters could be explained by the use of non-physiological conditions (absence of bilayer, low temperatures, proteins locked in particular conformational states). To address the molecular mechanism of ABC exporters under more physiological conditions LRET has been employed to study the conformational changes of functional MsbA. The bacterial ABC transporter MsbA has been used as a model for structural and functional studies of ABC exporters

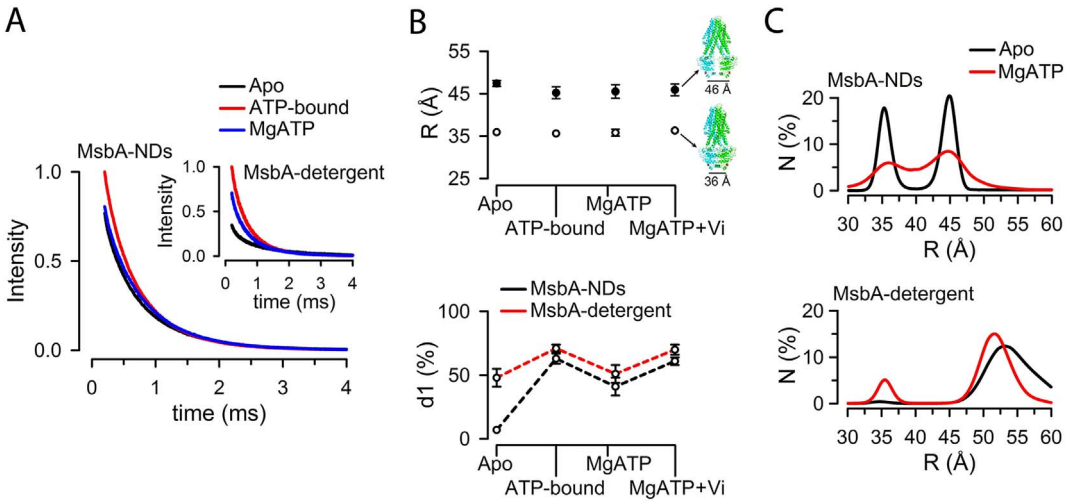

Fig. 8. Comparison of MsbA in NDs with MsbA in detergent. A. Sensitized Bodipy FL emission decays from MsbA in NDs (MsbA-NDs; main panel) and in detergent (MsbA-detergent; inset). Measurements were performed in the apo state (nucleotide free buffer with 1 mM EDTA to chelate trace divalent cations and prevent ATP hydrolysis) and after addition of NaATP (5 mM NaATP; ATP-bound state). Intensities were normalized to the ATP intensity at 200 μs. B. Top: distances calculated from the LRET sensitized Bodipy FL emission decays of MsbA-NDs. Possible structures associated with each distance are shown on the right (labeled C561 is shown in red). Measurements started in the apo state, and then the samples were analyzed after successive additions of ATP (5 mM NaATP; ATP-bound state), $MgSO_4$ (10 mM $MgSO_4$; MgATP; during continuous ATP hydrolysis) and sodium orthovanadate (0.25 mM Vi; MgATP + Vi state; post-hydrolysis intermediate state). Bottom: percentage of molecules with closely-associated NBDs (d1; ~36 Å). C. Distance distributions of MsbA in NDs (top) and in detergent (bottom). Distance distributions were calculated from the lifetime distributions of LRET sensitized emission intensity decays in the apo state and during hydrolysis. The MsbA T561C mutant was used in the experiments. Figures were adapted from reference [38], with permission from the American Society for Biochemistry and Molecular Biology.

[35,39,82,93,95,113–121]. It is a lipid flippase that uses the energy of ATP hydrolysis to translocate lipid A from the inner leaflet to the outer leaflet of the inner membrane of Gram-negative bacteria [114,120,121]. Lipid A is a component of the endotoxin responsible for the toxicity of Gram-negative bacteria [114,122].

MsbA (*S. typhimurium* MsbA) has a few advantages for LRET studies *vis-à-vis* Pgp and other mammalian ABC exporters: 1) it can be easily expressed in *E. coli*, 2) it has less native Cys that need to be removed to generate a Cys-less version, 3) since it is a homodimer, introduction of a single-Cys provides a pair of Cys in equivalent positions of the full transporter for LRET labeling, and 4) is quite stable in detergent. Although several single-Cys MsbA mutants have been studied, here we focus on the single-Cys mutant Thr561Cys; Thr561 is near the C-terminal end of the MsbA NBD. According to the MsbA structures and DEER spectroscopy, very large Cys561-Cys561 distance changes are expected during the MsbA hydrolysis cycle (Fig. 5A and B) [93,95]. Importantly, Cys561 is far away from the active site and it is accessible for labeling. MsbA-T561C displays a high ATPase activity, comparable to that of wild-type MsbA, which is not affected by labeling with the LRET donor or acceptor probes [35].

6.2. MsbA in detergent and NDs

MsbA purified by immobilized metal affinity chromatography and SEC is stable in salt buffers containing the detergents dodecylmaltoside (0.065%) and sodium cholate (0.04%) [35,39]. Addition of the latter greatly increases the functional stability of the protein stored at 4 °C. Different from the isolated NBDs, the purified homodimeric MsbA-T561C was labeled with the donor Tb^{3+} chelate and the fluorophore acceptor simultaneously [35,39]. The acceptor was N-(2-aminoethyl) maleimide (Bodipy FL maleimide) because the Förster distance for the Tb^{3+}-Bodipy FL pair of 41 Å provides very good sensitivity for the changes in distance that take place during hydrolysis. It is expected that LRET measurements will be from at most 50% of the labeled MsbA homodimers (those homodimers labeled with donor and acceptor). Random labeling is likely because the donor and acceptor reactions are based on the same maleimide-thiol chemistry and the same residue (Cys561) is labeled in each monomer. As a result, the other 50% of the MsbA molecules, donor/donor and acceptor/acceptor labeled, will be invisible to LRET.

Labeled MsbA can be studied in detergent or after reconstitution in liposomes or NDs. For reconstitution in NDs detergent-solubilized MsbA, *E. coli* lipids and MSP are mixed (Fig. 1) [39]. We have used MSP1E3D1, a MSP variant that produces empty NDs of ~11-nm diameter and MsbA-loaded NDs of ~13-nm diameter. These NDs fit one MsbA/ND, which was confirmed by SEC, dynamic light scattering and transmission electron microscopy. Even though empty NDs do not affect the LRET measurements, MsbA-loaded NDs can be purified by SEC or immobilized metal affinity chromatography [39]. Compared to MsbA in detergent, the ATPase activity of MsbA in NDs is 5 to 10 folds higher, and is less sensitive to changes in temperature [35,39]. A major advantage is that MsbA in NDs can be treated as a soluble protein.

6.3. Conformational changes on the MsbA NBDs side

Because of technical limitations and simplicity, most structural studies of MsbA and other ABC exporters have been performed with the proteins solubilized in detergent, locked in specific conformations and/or at low temperature [91–95]. However, studies under more physiological conditions are essential to understand the structure and function of ABC exporters. To this end, LRET in combination with reconstitution in NDs is very powerful since it allows for studies at 37 °C while the ABC exporters are functioning [39].

In general terms, the time course of the changes in LRET intensity in the different states is similar for MsbA and the isolated NBDs, meaning an increase in LRET with the transition from the apo (nucleotide-free, substrate-free) to the ATP-bound state, and a decrease during hydrolysis, after addition of Mg^{2+} (MgATP state; continuous hydrolysis at near maximal rate) [35,39]. Fig. 8A shows sensitized emission decays of MsbA in NDs (MsbA-NDs, main panel) and MsbA in detergent (MsbA-detergent, inset) in the apo state, ATP-bound state, and during ATP hydrolysis (MgATP state). It is clearly apparent that the increase in LRET intensity by transitioning from the apo state (black) to the ATP-bound state (red) is much reduced in the NDs. Also different from MsbA in detergent, in the NDs MsbA sensitized emission decay during hydrolysis (blue) is close to that of the apo state (black). Analysis of the MsbA LRET decays shows two dominant donor-acceptor distances in all cases, distances that remain unchanged during the ATP hydrolysis cycle

(Fig. 8B top). The shorter distance (~36 Å; d1) is essentially the same in NDs and detergent, and corresponds to the tightly-associated NBD dimer of the closed conformation (outward-facing) (Fig. 8B top). The longer Cys561-Cys561 distance (d2) is shorter in MsbA-ND (~47 Å) than in MsbA-detergent (~53 Å) [35,39], and much shorter than that in the inward-facing MsbA apo structure (> 80 Å; Figs. 5A, B and 8B top) [93]. The shorter d2 in detergent is not the result of constraints imposed by the ND because similar results were obtained for MsbA in ~100-nm diameter unilamellar liposomes [39].

The differences in LRET intensity decays are not caused by changes in distances (*i.e.*, different conformations), but changes in the percentage of molecules in each conformation [39]. Fig. 8B (bottom panel) shows the proportion of MsbA molecules (donor-acceptor pairs) adopting the 36-Å conformation (d1) during the ATP hydrolysis cycle for MsbA in NDs (black) and MsbA in detergent (red). The most striking difference is in the apo state, where the proportion of molecules in the 36-Å conformation is ~50% in MsbA-ND *vs.* only < 10% in MsbA-detergent. This observation suggests that reconstitution of MsbA into a lipid bilayer shifts the equilibrium towards associated NBDs, even in the absence of nucleotide.

Analysis of LRET intensity decays also yields distance distributions, which are useful to discriminate discrete from continuous distributions between conformations. The results confirm the presence of discrete conformations in MsbA-ND in all the states studied, except for the most physiological, MsbA in ND during ATP hydrolysis (Fig. 8C, top, red) [39]. This broadening of the distance distribution during hydrolysis is not present in MsbA-detergent (Fig. 8C, bottom, red) [39]. Also, MsbA in detergent samples much longer distances in the apo state than MsbA in NDs (Fig. 8C, black, bottom *vs.* top) [39]. This suggests high flexibility of the apo MsbA in detergent micelles. Overall, the distance distributions in Fig. 8C show that MsbA is more compact in NDs than in detergent [39]. Basically, the main differences between LRET in MsbA-ND and MsbA-detergent are: 1) a much larger fraction of NBDs associated or in very close proximity in the apo MsbA-ND, and 2) the replacement of the longer distance of fully-dissociated NBDs in MsbA-detergent by a shorter distance compatible with loosely-associated NBDs or NBDs dissociated, but very close to each other. It seems that the catalytic cycle of MsbA reconstituted in a lipid bilayer proceeds with smaller conformational changes than previously thought, in agreement with a FRET study of Pgp in liposomes at 37 °C, electron-microscopy of Pgp showing close proximity of the NBDs in apo state, and computational studies [96,123–125].

7. Concluding remarks

LRET is a powerful technique that can be used to follow conformational changes in real time with atomic resolution. The studies on isolated NBDs show that occupancy of both NBSs is needed to form a dimer, whereas dissociation of the dimer follows hydrolysis of only one of the two ATPs bound. Conformational changes on the NBD side of the ABC exporters switch the accessibility of the substrate-binding pocket between the inside and outside, which is coupled to substrate transport. However, the magnitude and nature of the changes at the NBD side that drive the alternating access are not well defined. The results on MsbA studied under near-physiological conditions show that the conformational changes during the ATP hydrolysis cycle are much smaller than previously thought; the NBDs separate by only ~10 Å. It seems likely that the large NBD to NBD distances of MsbA crystal structures represent rare conformations. The results using LRET on MsbA reconstituted in NDs stress the importance of performing structural/functional studies of ABC exporters under conditions as close as native as possible, including, at a minimum, reconstitution into lipid bilayers and normal temperatures.

Conflict of interest

The authors declare no conflict of interest.

Abbreviations

ABC	ATP-binding cassette
CFTR	Cystic fibrosis transmembrane conductance regulator; ABCC7
DEER	double electron-electron resonance
FRET	Förster (or fluorescence) resonance energy transfer
LRET	Lanthanide (or luminescence) resonance energy transfer
MP	Membrane protein
MRP1	Multidrug resistance protein 1; ABCC1
NBD	Nucleotide binding domain
NBS	Nucleotide binding site
ND	Nanodisc
Pgp	P-glycoprotein; MDR1; ABCB1
SMALP	Styrene-maleic acid (SMA)-lipid particle; Lipodisq
TMD	Transmembrane domain

Transparency document

The http://dx.doi.org/10.1016/j.bbamem.2017.08.005 associated with this article can be found, in online version.

Acknowledgements

This work was supported by the TTUHSC Center for Membrane Protein Research, Cancer Prevention and Research Institute of Texas Grant RP101073, and National Institutes of Health Grants R01GM79629 and 3R01GM079629-03S1.

References

[1] E. Wallin, G. von Heijne, Genome-wide analysis of integral membrane proteins from eubacterial, archaean, and eukaryotic organisms, Protein Sci. 7 (1998) 1029–1038.
[2] D. Keppler, Export pumps for glutathione S-conjugates, Free Radic. Biol. Med. 27 (1999) 985–991.
[3] R.S. Cantor, Lipid composition and the lateral pressure profile in bilayers, Biophys. J. 76 (1999) 2625–2639.
[4] M.F. Brown, Curvature forces in membrane lipid-protein interactions, Biochemistry 51 (2012) 9782–9795.
[5] O.S. Andersen, R.E. Koeppe, Bilayer thickness and membrane protein function: an energetic perspective, Annu. Rev. Biophys. Biomol. Struct. 36 (2007) 107–130.
[6] R. Phillips, T. Ursell, P. Wiggins, P. Sens, Emerging roles for lipids in shaping membrane-protein function, Nature 459 (2009) 379–385.
[7] M. Etzkorn, T. Raschle, F. Hagn, V. Gelev, A.J. Rice, T. Walz, G. Wagner, Cell-free expressed bacteriorhodopsin in different soluble membrane mimetics: biophysical properties and NMR accessibility, Structure 21 (2013) 394–401.
[8] R.B. Rues, V. Dotsch, F. Bernhard, Co-translational formation and pharmacological characterization of beta1-adrenergic receptor/nanodisc complexes with different lipid environments, Biochim. Biophys. Acta 1858 (2016) 1306–1316.
[9] A. Patist, J.R. Kanicky, P.K. Shukla, D.O. Shah, Importance of micellar kinetics in relation to technological processes, J. Colloid Interface Sci. 245 (2002) 1–15.
[10] J.A. Whiles, R. Deems, R.R. Vold, E.A. Dennis, Bicelles in structure-function studies of membrane-associated proteins, Bioorg. Chem. 30 (2002) 431–442.
[11] T.H. Bayburt, S.G. Sligar, Membrane protein assembly into Nanodiscs, FEBS Lett. 584 (2010) 1721–1727.
[12] I.G. Denisov, S.G. Sligar, Nanodiscs for structural and functional studies of membrane proteins, Nat. Struct. Mol. Biol. 23 (2016) 481–486.
[13] M.A. Schuler, I.G. Denisov, S.G. Sligar, Nanodiscs as a new tool to examine lipid-protein interactions, Methods Mol. Biol. 974 (2013) 415–433.
[14] S. Inagaki, R. Ghirlando, R. Grisshammer, Biophysical characterization of membrane proteins in nanodiscs, Methods 59 (2013) 287–300.
[15] F. Hagn, M. Etzkorn, T. Raschle, G. Wagner, Optimized phospholipid bilayer nanodiscs facilitate high-resolution structure determination of membrane proteins, J. Am. Chem. Soc. 135 (2013) 1919–1925.
[16] N. Skar-Gislinge, J.B. Simonsen, K. Mortensen, R. Feidenhans'l, S.G. Sligar, B. Lindberg Moller, T. Bjornholm, L. Arleth, Elliptical structure of phospholipid bilayer nanodiscs encapsulated by scaffold proteins: casting the roles of the lipids and the protein, J. Am. Chem. Soc. 132 (2010) 13713–13722.
[17] I.G. Denisov, Y.V. Grinkova, A.A. Lazarides, S.G. Sligar, Directed self-assembly of monodisperse phospholipid bilayer Nanodiscs with controlled size, J. Am. Chem. Soc. 126 (2004) 3477–3487.

[18] T.K. Ritchie, Y.V. Grinkova, T.H. Bayburt, I.G. Denisov, J.K. Zolnerciks, W.M. Atkins, S.G. Sligar, Chapter 11 - reconstitution of membrane proteins in phospholipid bilayer nanodiscs, Methods Enzymol. 464 (2009) 211–231.
[19] J.M. Dorr, S. Scheidelaar, M.C. Koorengevel, J.J. Dominguez, M. Schafer, C.A. van Walree, J.A. Killian, The styrene-maleic acid copolymer: a versatile tool in membrane research, Eur. Biophys. J. 45 (2016) 3–21.
[20] M. Jamshad, Y.P. Lin, T.J. Knowles, R.A. Parslow, C. Harris, M. Wheatley, D.R. Poyner, R.M. Bill, O.R. Thomas, M. Overduin, T.R. Dafforn, Surfactant-free purification of membrane proteins with intact native membrane environment, Biochem. Soc. Trans. 39 (2011) 813–818.
[21] T.J. Knowles, R. Finka, C. Smith, Y.P. Lin, T. Dafforn, M. Overduin, Membrane proteins solubilized intact in lipid containing nanoparticles bounded by styrene maleic acid copolymer, J. Am. Chem. Soc. 131 (2009) 7484–7485.
[22] S. Banerjee, K. Sen, T.K. Pal, S.K. Guha, Poly(styrene-co-maleic acid)-based pH-sensitive liposomes mediate cytosolic delivery of drugs for enhanced cancer chemotherapy, Int. J. Pharm. 436 (2012) 786–797.
[23] A.J. Rothnie, Detergent-free membrane protein purification, Methods Mol. Biol. 1432 (2016) 261–267.
[24] A.O. Oluwole, B. Danielczak, A. Meister, J.O. Babalola, C. Vargas, S. Keller, Solubilization of membrane proteins into functional lipid-bilayer nanodiscs using a diisobutylene/maleic acid copolymer, Angew. Chem. Int. Ed. Engl. 56 (2017) 1919–1924.
[25] J.R. Lakowicz, Principles of Fluorescence Spectroscopy, Springer, New York, 2006.
[26] P.R. Selvin, Principles and biophysical applications of lanthanide-based probes, Annu. Rev. Biophys. Biomol. Struct. 31 (2002) 275–302.
[27] T. Heyduk, Luminescence resonance energy transfer analysis of RNA polymerase complexes, Methods 25 (2001) 44–53.
[28] M.E. Zoghbi, S. Krishnan, G.A. Altenberg, Dissociation of ATP-binding cassette nucleotide-binding domain dimers into monomers during the hydrolysis cycle, J. Biol. Chem. 287 (2012) 14994–15000.
[29] X. Bao, S.C. Lee, L. Reuss, G.A. Altenberg, Change in permeant size selectivity by phosphorylation of connexin 43 gap-junctional hemichannels by PKC, Proc. Natl. Acad. Sci. U. S. A. 104 (2007) 4919–4924.
[30] P. Ge, P.R. Selvin, Carbostyril derivatives as antenna molecules for luminescent lanthanide chelates, Bioconjug. Chem. 15 (2004) 1088–1094.
[31] K. Barthelmes, A.M. Reynolds, E. Peisach, H.R. Jonker, N.J. DeNunzio, K.N. Allen, B. Imperiali, H. Schwalbe, Engineering encodable lanthanide-binding tags into loop regions of proteins, J. Am. Chem. Soc. 133 (2011) 808–819.
[32] M. Nitz, K.J. Franz, R.L. Maglathlin, B. Imperiali, A powerful combinatorial screen to identify high-affinity terbium(III)-binding peptides, Chembiochem 4 (2003) 272–276.
[33] W. Sandtner, F. Bezanilla, A.M. Correa, In vivo measurement of intramolecular distances using genetically encoded reporters, Biophys. J. 93 (2007) L45–47.
[34] W. Sandtner, B. Egwolf, F. Khalili-Araghi, J.E. Sanchez-Rodriguez, B. Roux, F. Bezanilla, M. Holmgren, Ouabain binding site in a functioning Na^+/K^+ ATPase, J. Biol. Chem. 286 (2011) 38177–38183.
[35] R.S. Cooper, G.A. Altenberg, Association/dissociation of the nucleotide-binding domains of the ATP-binding cassette protein MsbA measured during continuous hydrolysis, J. Biol. Chem. 288 (2013) 20785–20796.
[36] D.J. Swartz, L. Mok, S.K. Botta, A. Singh, G.A. Altenberg, I.L. Urbatsch, Directed evolution of P-glycoprotein cysteines reveals site-specific, non-conservative substitutions that preserve multidrug resistance, Biosci. Rep. 34 (2014).
[37] P. Ge, P.R. Selvin, Thiol-reactive luminescent lanthanide chelates: part 2, Bioconjug. Chem. 14 (2003) 870–876.
[38] J. Chen, P.R. Selvin, Thiol-reactive luminescent chelates of terbium and europium, Bioconjug. Chem. 10 (1999) 311–315.
[39] M.E. Zoghbi, R.S. Cooper, G.A. Altenberg, The lipid bilayer modulates the structure and function of an ATP-binding cassette exporter, J. Biol. Chem. 291 (2016) 4453–4461.
[40] M.E. Zoghbi, G.A. Altenberg, ATP binding to two sites is necessary for dimerization of nucleotide-binding domains of ABC proteins, Biochem. Biophys. Res. Commun. 443 (2014) 97–102.
[41] M.E. Zoghbi, G.A. Altenberg, Hydrolysis at one of the two nucleotide-binding sites drives the dissociation of ATP-binding cassette nucleotide-binding domain dimers, J. Biol. Chem. 288 (2013) 34259–34265.
[42] D.J. Posson, P.R. Selvin, Extent of voltage sensor movement during gating of shaker K^+ channels, Neuron 59 (2008) 98–109.
[43] D.J. Posson, P. Ge, C. Miller, F. Bezanilla, P.R. Selvin, Small vertical movement of a K^+ channel voltage sensor measured with luminescence energy transfer, Nature 436 (2005) 848–851.
[44] H.C. Hyde, W. Sandtner, E. Vargas, A.T. Dagcan, J.L. Robertson, B. Roux, A.M. Correa, F. Bezanilla, Nano-positioning system for structural analysis of functional homomeric proteins in multiple conformations, Structure 20 (2012) 1629–1640.
[45] A. Muschielok, J. Michaelis, Application of the nano-positioning system to the analysis of fluorescence resonance energy transfer networks, J. Phys. Chem. B 115 (2011) 11927–11937.
[46] A. Muschielok, J. Andrecka, A. Jawhari, F. Bruckner, P. Cramer, J. Michaelis, A nano-positioning system for macromolecular structural analysis, Nat. Methods 5 (2008) 965–971.
[47] T. Kubota, T. Durek, B. Dang, R.K. Finol-Urdaneta, D.J. Craik, S.B. Kent, R.J. French, F. Bezanilla, A.M. Correa, Mapping of voltage sensor positions in resting and inactivated mammalian sodium channels by LRET, Proc. Natl. Acad. Sci. U. S. A. 114 (2017) E1857–E1865.
[48] D. Barthelmes, K. Barthelmes, K. Schnorr, H.R.A. Jonker, B. Bodmer, K.N. Allen, B. Imperiali, H. Schwalbe, Conformational dynamics and alignment properties of loop lanthanide-binding-tags (LBTs) studied in interleukin-1beta, J. Biomol. NMR (2017).
[49] R.Y. Tsien, Breeding and building molecules to spy on cells and tumors, Keio J. Med. 55 (2006) 127–140.
[50] G. Crivat, J.W. Taraska, Imaging proteins inside cells with fluorescent tags, Trends Biotechnol. 30 (2012) 8–16.
[51] A. Siemiarczuk, B.D. Wagner, W.R. Ware, Comparison of the maximum entropy and exponential series methods for the recovery of distributions of lifetimes from fluorescence lifetime data, J. Phys. Chem. 94 (1990) 1661–1666.
[52] D.R. James, W.R. Ware, Recovery of underlying distributions of lifetimes from fluorescence decay data, Chem. Phys. Lett. 126 (1986) 7–11.
[53] A. Cha, G.E. Snyder, P.R. Selvin, F. Bezanilla, Atomic scale movement of the voltage-sensing region in a potassium channel measured via spectroscopy, Nature 402 (1999) 809–813.
[54] J. Gonzalez, M. Du, K. Parameshwaran, V. Suppiramaniam, V. Jayaraman, Role of dimer interface in activation and desensitization in AMPA receptors, Proc. Natl. Acad. Sci. U. S. A. 107 (2010) 9891–9896.
[55] S.S. Ramaswamy, D.M. MacLean, A.A. Gorfe, V. Jayaraman, Proton-mediated conformational changes in an acid-sensing ion channel, J. Biol. Chem. 288 (2013) 35896–35903.
[56] A. Rambhadran, J. Gonzalez, V. Jayaraman, Subunit arrangement in *N*-methyl-D-aspartate (NMDA) receptors, J. Biol. Chem. 285 (2010) 15296–15301.
[57] R.E. Sirrieh, D.M. MacLean, V. Jayaraman, Amino-terminal domain tetramer organization and structural effects of zinc binding in the *N*-methyl-D-aspartate (NMDA) receptor, J. Biol. Chem. 288 (2013) 22555–22564.
[58] P.A. Knauf, P. Pal, Use of luminescence resonance energy transfer to measure distances in the AE1 anion exchange protein dimer, Blood Cells Mol. Dis. 32 (2004) 360–365.
[59] P. Pal, B.E. Holmberg, P.A. Knauf, Conformational changes in the cytoplasmic domain of human anion exchanger 1 revealed by luminescence resonance energy transfer, Biochemistry 44 (2005) 13638–13649.
[60] E.V. Sineva, J.A. Rumfeldt, J.R. Halpert, D.R. Davydov, A large-scale allosteric transition in cytochrome P450 3A4 revealed by luminescence resonance energy transfer (LRET), PLoS One 8 (2013) e83898.
[61] P. Bouige, D. Laurent, L. Piloyan, E. Dassa, Phylogenetic and functional classification of ATP-binding cassette (ABC) systems, Curr. Protein Pept. Sci. 3 (2002) 541–559.
[62] F.J. Sharom, ABC multidrug transporters: structure, function and role in chemoresistance, Pharmacogenomics 9 (2008) 105–127.
[63] M.K. Al-Shawi, Catalytic and transport cycles of ABC exporters, Essays Biochem. 50 (2011) 63–83.
[64] K.P. Locher, Mechanistic diversity in ATP-binding cassette (ABC) transporters, Nat. Struct. Mol. Biol. 23 (2016) 487–493.
[65] A.J. Slot, S.V. Molinski, S.P. Cole, Mammalian multidrug-resistance proteins (MRPs), Essays Biochem. 50 (2011) 179–207.
[66] J. Bryan, A. Munoz, X. Zhang, M. Dufer, G. Drews, P. Krippeit-Drews, L. Aguilar-Bryan, ABCC8 and ABCC9: ABC transporters that regulate K^+ channels, Pflugers Arch. 453 (2007) 703–718.
[67] S. Hulpke, M. Tomioka, E. Kremmer, K. Ueda, R. Abele, R. Tampe, Direct evidence that the N-terminal extensions of the TAP complex act as autonomous interaction scaffolds for the assembly of the MHC I peptide-loading complex, Cell. Mol. Life Sci. 69 (2012) 3317–3327.
[68] Z.L. Johnson, J. Chen, Structural basis of substrate recognition by the multidrug resistance protein MRP1, Cell 168 (2017) 1075–1085 (e1079).
[69] A. Mahringer, G. Fricker, ABC transporters at the blood-brain barrier, Expert Opin. Drug Metab. Toxicol. 12 (2016) 499–508.
[70] A.A. Joshi, S.S. Vaidya, M.V. St-Pierre, A.M. Mikheev, K.E. Desino, A.N. Nyandege, K.L. Audus, J.D. Unadkat, P.M. Gerk, Placental ABC transporters: biological impact and pharmaceutical significance, Pharm. Res. 33 (2016) 2847–2878.
[71] A. Tamaki, C. Ierano, G. Szakacs, R.W. Robey, S.E. Bates, The controversial role of ABC transporters in clinical oncology, Essays Biochem. 50 (2011) 209–232.
[72] P.C. Smith, N. Karpowich, L. Millen, J.E. Moody, J. Rosen, P.J. Thomas, J.F. Hunt, ATP binding to the motor domain from an ABC transporter drives formation of a nucleotide sandwich dimer, Mol. Cell 10 (2002) 139–149.
[73] E. Procko, I. Ferrin-O'Connell, S.L. Ng, R. Gaudet, Distinct structural and functional properties of the ATPase sites in an asymmetric ABC transporter, Mol. Cell 24 (2006) 51–62.
[74] N. Grossmann, A.S. Vakkasoglu, S. Hulpke, R. Abele, R. Gaudet, R. Tampe, Mechanistic determinants of the directionality and energetics of active export by a heterodimeric ABC transporter, Nat. Commun. 5 (2014) 5419.
[75] M. Hohl, L.M. Hurlimann, S. Bohm, J. Schoppe, M.G. Grutter, E. Bordignon, M.A. Seeger, Structural basis for allosteric cross-talk between the asymmetric nucleotide binding sites of a heterodimeric ABC exporter, Proc. Natl. Acad. Sci. U. S. A. 111 (2014) 11025–11030.
[76] W. Huang, J.L. Liao, Catalytic mechanism of the maltose transporter hydrolyzing ATP, Biochemistry 55 (2016) 224–231.
[77] S.P. Cole, Multidrug resistance protein 1 (MRP1, ABCC1), a "multitasking" ATP-binding cassette (ABC) transporter, J. Biol. Chem. 289 (2014) 30880–30888.
[78] E.M. Leslie, R.G. Deeley, S.P. Cole, Multidrug resistance proteins: role of P-glycoprotein, MRP1, MRP2, and BCRP (ABCG2) in tissue defense, Toxicol. Appl. Pharmacol. 204 (2005) 216–237.
[79] Z.E. Sauna, I.W. Kim, K. Nandigama, S. Kopp, P. Chiba, S.V. Ambudkar, Catalytic cycle of ATP hydrolysis by P-glycoprotein: evidence for formation of the E.S reaction intermediate with ATP-gamma-S, a nonhydrolyzable analogue of ATP, Biochemistry 46 (2007) 13787–13799.
[80] L. Esser, F. Zhou, K.M. Pluchino, J. Shiloach, J. Ma, W.K. Tang, C. Gutierrez,

A. Zhang, S. Shukla, J.P. Madigan, T. Zhou, P.D. Kwong, S.V. Ambudkar, M.M. Gottesman, D. Xia, Structures of the multidrug transporter P-glycoprotein reveal asymmetric ATP binding and the mechanism of polyspecificity, J. Biol. Chem. 292 (2017) 446–461.
[81] A. Siarheyeva, R. Liu, F.J. Sharom, Characterization of an asymmetric occluded state of P-glycoprotein with two bound nucleotides: implications for catalysis, J. Biol. Chem. 285 (2010) 7575–7586.
[82] A. Mittal, S. Bohm, M.G. Grutter, E. Bordignon, M.A. Seeger, Asymmetry in the homodimeric ABC transporter MsbA recognized by a DARPin, J. Biol. Chem. 287 (2012) 20395–20406.
[83] A.E. Senior, M.K. al-Shawi, I.L. Urbatsch, The catalytic cycle of P-glycoprotein, FEBS Lett. 377 (1995) 285–289.
[84] K.P. Hopfner, A. Karcher, D.S. Shin, L. Craig, L.M. Arthur, J.P. Carney, J.A. Tainer, Structural biology of Rad50 ATPase: ATP-driven conformational control in DNA double-strand break repair and the ABC-ATPase superfamily, Cell 101 (2000) 789–800.
[85] J. Chen, G. Lu, J. Lin, A.L. Davidson, F.A. Quiocho, A tweezers-like motion of the ATP-binding cassette dimer in an ABC transport cycle, Mol. Cell 12 (2003) 651–661.
[86] C.F. Higgins, Multiple molecular mechanisms for multidrug resistance transporters, Nature 446 (2007) 749–757.
[87] E. Janas, M. Hofacker, M. Chen, S. Gompf, C. van der Does, R. Tampe, The ATP hydrolysis cycle of the nucleotide-binding domain of the mitochondrial ATP-binding cassette transporter Mdl1p, J. Biol. Chem. 278 (2003) 26862–26869.
[88] P. Vergani, S.W. Lockless, A.C. Nairn, D.C. Gadsby, CFTR channel opening by ATP-driven tight dimerization of its nucleotide-binding domains, Nature 433 (2005) 876–880.
[89] R.J. Dawson, K.P. Locher, Structure of a bacterial multidrug ABC transporter, Nature 443 (2006) 180–185.
[90] C. Oswald, I.B. Holland, L. Schmitt, The motor domains of ABC-transporters. What can structures tell us? Naunyn Schmiedeberg's Arch. Pharmacol. 372 (2006) 385–399.
[91] J. Li, K.F. Jaimes, S.G. Aller, Refined structures of mouse P-glycoprotein, Protein Sci. 23 (2014) 34–46.
[92] S.G. Aller, J. Yu, A. Ward, Y. Weng, S. Chittaboina, R. Zhuo, P.M. Harrell, Y.T. Trinh, Q. Zhang, I.L. Urbatsch, G. Chang, Structure of P-glycoprotein reveals a molecular basis for poly-specific drug binding, Science 323 (2009) 1718–1722.
[93] A. Ward, C.L. Reyes, J. Yu, C.B. Roth, G. Chang, Flexibility in the ABC transporter MsbA: alternating access with a twist, Proc. Natl. Acad. Sci. U. S. A. 104 (2007) 19005–19010.
[94] B. Verhalen, R. Dastvan, S. Thangapandian, Y. Peskova, H.A. Koteiche, R.K. Nakamoto, E. Tajkhorshid, H.S. McHaourab, Energy transduction and alternating access of the mammalian ABC transporter P-glycoprotein, Nature 543 (2017) 738–741.
[95] P. Zou, M. Bortolus, H.S. McHaourab, Conformational cycle of the ABC transporter MsbA in liposomes: detailed analysis using double electron-electron resonance spectroscopy, J. Mol. Biol. 393 (2009) 586–597.
[96] J.Y. Lee, I.L. Urbatsch, A.E. Senior, S. Wilkens, Nucleotide-induced structural changes in P-glycoprotein observed by electron microscopy, J. Biol. Chem. 283 (2008) 5769–5779.
[97] B. Verhalen, S. Wilkens, P-glycoprotein retains drug-stimulated ATPase activity upon covalent linkage of the two nucleotide binding domains at their C-terminal ends, J. Biol. Chem. 286 (2011) 10476–10482.
[98] T.W. Loo, M.C. Bartlett, D.M. Clarke, Drug binding in human P-glycoprotein causes conformational changes in both nucleotide-binding domains, J. Biol. Chem. 278 (2003) 1575–1578.
[99] L. Pan, S.G. Aller, Equilibrated atomic models of outward-facing P-glycoprotein and effect of ATP binding on structural dynamics, Sci. Rep. 5 (2015) 7880.
[100] A. Moeller, S.C. Lee, H. Tao, J.A. Speir, G. Chang, I.L. Urbatsch, C.S. Potter, B. Carragher, Q. Zhang, Distinct conformational spectrum of homologous multidrug ABC transporters, Structure 23 (2015) 450–460.
[101] S. Narita, H. Tokuda, An ABC transporter mediating the membrane detachment of bacterial lipoproteins depending on their sorting signals, FEBS Lett. 580 (2006) 1164–1170.
[102] J.E. Moody, L. Millen, D. Binns, J.F. Hunt, P.J. Thomas, Cooperative, ATP-dependent association of the nucleotide binding cassettes during the catalytic cycle of ATP-binding cassette transporters, J. Biol. Chem. 277 (2002) 21111–21114.
[103] Y.R. Yuan, S. Blecker, O. Martsinkevich, L. Millen, P.J. Thomas, J.F. Hunt, The crystal structure of the MJ0796 ATP-binding cassette. Implications for the structural consequences of ATP hydrolysis in the active site of an ABC transporter, J. Biol. Chem. 276 (2001) 32313–32321.
[104] G.A. Fendley, I.L. Urbatsch, R.B. Sutton, M.E. Zoghbi, G.A. Altenberg, Nucleotide dependence of the dimerization of ATP binding cassette nucleotide binding domains, Biochem. Biophys. Res. Commun. 480 (2016) 268–272.
[105] M.E. Zoghbi, K.L. Fuson, R.B. Sutton, G.A. Altenberg, Kinetics of the association/dissociation cycle of an ATP-binding cassette nucleotide-binding domain, J. Biol. Chem. 287 (2012) 4157–4164.
[106] V. Kayser, N. Chennamsetty, V. Voynov, B. Helk, B.L. Trout, Tryptophan-tryptophan energy transfer and classification of tryptophan residues in proteins using a therapeutic monoclonal antibody as a model, J. Fluoresc. 21 (2011) 275–288.
[107] R.F. Chen, J.R. Knutson, H. Ziffer, D. Porter, Fluorescence of tryptophan dipeptides: correlations with the rotamer model, Biochemistry 30 (1991) 5184–5195.
[108] G.B. McGaughey, M. Gagne, A.K. Rappe, pi-Stacking interactions. Alive and well in proteins, J. Biol. Chem. 273 (1998) 15458–15463.
[109] G. Gyimesi, S. Ramachandran, P. Kota, N.V. Dokholyan, B. Sarkadi, T. Hegedus, ATP hydrolysis at one of the two sites in ABC transporters initiates transport related conformational transitions, Biochim. Biophys. Acta 1808 (2011) 2954–2964.
[110] P.C. Wen, E. Tajkhorshid, Dimer opening of the nucleotide binding domains of ABC transporters after ATP hydrolysis, Biophys. J. 95 (2008) 5100–5110.
[111] P.M. Jones, A.M. George, Opening of the ADP-bound active site in the ABC transporter ATPase dimer: evidence for a constant contact, alternating sites model for the catalytic cycle, Proteins 75 (2009) 387–396.
[112] P.M. Jones, M.L. O'Mara, A.M. George, ABC transporters: a riddle wrapped in a mystery inside an enigma, Trends Biochem. Sci. 34 (2009) 520–531.
[113] H. Singh, S. Velamakanni, M.J. Deery, J. Howard, S.L. Wei, H.W. van Veen, ATP-dependent substrate transport by the ABC transporter MsbA is proton-coupled, Nat. Commun. 7 (2016) 12387.
[114] G. King, F.J. Sharom, Proteins that bind and move lipids: MsbA and NPC1, Crit. Rev. Biochem. Mol. Biol. 47 (2012) 75–95.
[115] P.D. Eckford, F.J. Sharom, The reconstituted *Escherichia coli* MsbA protein displays lipid flippase activity, Biochem. J. 429 (2010) 195–203.
[116] P. Zou, H.S. McHaourab, Alternating access of the putative substrate-binding chamber in the ABC transporter MsbA, J. Mol. Biol. 393 (2009) 574–585.
[117] A. Siarheyeva, F.J. Sharom, The ABC transporter MsbA interacts with lipid A and amphipathic drugs at different sites, Biochem. J. 419 (2009) 317–328.
[118] P.P. Borbat, K. Surendhran, M. Bortolus, P. Zou, J.H. Freed, H.S. McHaourab, Conformational motion of the ABC transporter MsbA induced by ATP hydrolysis, PLoS Biol. 5 (2007) e271.
[119] J. Dong, G. Yang, H.S. McHaourab, Structural basis of energy transduction in the transport cycle of MsbA, Science 308 (2005) 1023–1028.
[120] W.T. Doerrler, H.S. Gibbons, C.R. Raetz, MsbA-dependent translocation of lipids across the inner membrane of *Escherichia coli*, J. Biol. Chem. 279 (2004) 45102–45109.
[121] W.T. Doerrler, C.R. Raetz, ATPase activity of the MsbA lipid flippase of *Escherichia coli*, J. Biol. Chem. 277 (2002) 36697–36705.
[122] X. Wang, P.J. Quinn, A. Yan, Kdo2 -lipid A: structural diversity and impact on immunopharmacology, Biol. Rev. Camb. Philos. Soc. 90 (2015) 408–427.
[123] B. Verhalen, S. Ernst, M. Borsch, S. Wilkens, Dynamic ligand-induced conformational rearrangements in P-glycoprotein as probed by fluorescence resonance energy transfer spectroscopy, J. Biol. Chem. 287 (2012) 1112–1127.
[124] P.M. Jones, A.M. George, Molecular-dynamics simulations of the ATP/apo state of a multidrug ATP-binding cassette transporter provide a structural and mechanistic basis for the asymmetric occluded state, Biophys. J. 100 (2011) 3025–3034.
[125] P.M. Jones, A.M. George, Nucleotide-dependent allostery within the ABC transporter ATP-binding cassette: a computational study of the MJ0796 dimer, J. Biol. Chem. 282 (2007) 22793–22803.